

Orsay LPTHE-96-85
Saclay SPhT-T96/050
Strasbourg LPT-96-21

Phenomenology of supersymmetric models with a singlet ¹

U. Ellwanger

LPTHE, Université de Paris-Sud, F-91400 Orsay

M. Rausch de Traubenberg

Laboratoire de Physique Théorique, Université Louis Pasteur,
Strasbourg

C.A. Savoy

Service de Physique Théorique, C. E. de Saclay, F-91191 Gif-sur-Yvette

Abstract

The supersymmetric extension of the standard model with an additional gauge singlet is analysed in detail in the light of the recent experimental bounds on supersymmetric particles. The useful part of the parameter space and the particle spectrum are displayed. We find that once the recent bounds on the chargino mass are imposed, all other new particles practically satisfy the present experimental limits. Special attention is given to particles to be searched for in the future experiments. The singlet fields tend to decouple and give rise to an effective MSSM, enlarging the validity of many phenomenological analyses based in the minimal field content. However, in some ranges of the parameters the singlino is the lightest neutralino, which modifies the signature for susy particles. Simple analytical approximations are developed that qualitatively explain the numerical results.

¹Supported in part by the EC grant Flavourdynamics.

1 Introduction

The addition of a $SU(3) \times SU(2) \times U(1)$ gauge singlet supermultiplet to the MSSM (minimal supersymmetric extension of the Standard Model) has been motivated by several issues: (i) the solution of the so-called μ -problem; (ii) the possibility of spontaneous breaking of the CP symmetry; (iii) the upper limits on the Higgs mass that are relatively low in the MSSM could be relaxed; (iv) the neutral particle spectrum is enriched by two scalars and one fermion, which could mix with other Higgs bosons and neutralinos and modify their physical properties; (v) possible deviations from the MSSM could urge to enlarge the experimental searches, which have been centred upon the MSSM. We refer here to the supersymmetric model with a gauge singlet in its simplest version, as defined below, as the (M+1)SSM.

However, according to our analysis, the strong constraints from LEP experiments, when combined with theoretical and phenomenological requirements, select the (M+1)SSM parameters in such a way that the gauge singlet scalars and fermions are basically decoupled and the rest of the spectrum effectively reproduces a restricted class of the MSSM. Because of this similarity, the motivations (ii)-(v) fade out as these issues are excluded or diminished after such a detailed investigation. Nevertheless, this also means that phenomenological analyses of the MSSM apply to a large extent to the (M+1)SSM as well! Still, if supersymmetry is found, one can go further and look for some peculiarities that could distinguish the two kind of models, specially in the case in which the lightest supersymmetric particle is the singlet fermion, or singlino. The (M+1)SSM can also be experimentally tested from the fact that the effective parameters in the equivalent MSSM are very constrained.

The present paper is devoted to a thorough discussion of the model in its version with only dimensionless couplings in its superpotential, and universal boundary conditions for the soft supersymmetric breaking terms at the GUT scale. With these assumptions, the dimensionality of the parameter space of the (M+1)SSM equals that of the MSSM. Our aim is to understand the pattern of the particle spectrum, correlations among the particle masses, and features which are in common with or different from the MSSM. An analysis of the complete parameters space of the model requires numerical methods, as a scanning over the independent parameters at the GUT scale, their subsequent evolution using the RGE down to the weak scale, the minimization of the Higgs potential, the implementation of theoretical and experimental constraints and finally the computation of the particle masses and some mixing angles.

Many phenomenological analyses of the model have appeared before [1, 2, 3, 4, 5]. The purpose of the present work is twofold. First, we implement the most recent experimental constraints on sparticles, Higgs and top quark masses from the LEP and the Tevatron [6, 7]. Second, we explain the

results of our numerical procedure with the help of analytic approximations and inequalities among the parameters. Once the vacua which break colour, electromagnetism or correspond to $\tan\beta = \infty$ are forbidden and the experimental constraints are imposed, these formulae allow us to understand the essential features of the bounds on and correlations among some particle masses. Quite a lot of attention is paid to the property found in [2], namely, that the singlet scalar acquires a v.e.v. which is much larger than the Higgs ones. Indeed, this has the important consequence that the singlet fermion and scalars quite decouple from the other multiplets as already mentioned.

In section 2 we review the motivations for the model, its essential differences with respect to the MSSM due to the enlargement of Higgs sector and the status of the spontaneous CP violation. The universality assumption for the soft terms and some of its consequences are explained in section 3. Section 4 contains the minimum conditions for the scalar potential as well as the scalar Higgs masses with the radiative corrections included in an approximation that is generally good, though we use the full expressions [8] in our numerical calculations. In section 5 we derive some approximate constraints from the stability of the vacuum to understand the pattern of the physical predictions. In section 6 we discuss some correlations in the mass spectrum along the same approximations. Then we summarize our implementation of the experimental and theoretical constraints on the model, in section 7. The main results of the careful scanning of the parameter space are displayed in the figures in section 8, with some emphasis on the sparticles more likely to be discovered at the colliders, with the exception of the Higgs sector that has been already presented [5]. The results are summarized in the last section. Some useful solutions of the RGE for the soft terms (with generic boundary conditions, for completeness) are listed in the Appendix.

2 General properties of the (M+1)SSM

The superpotential of the (M+1)SSM (where family mixing is neglected and irrelevant for the analysis in this paper) is given by

$$\begin{aligned}
 W = & \lambda S H_1 H_2 + \frac{\kappa}{3} S^3 + h_t T H_2 Q_3 + h_b B H_1 Q_3 + h_\tau E H_1 L \\
 & + (\text{similar terms for the lighter quarks and leptons}) \quad (1)
 \end{aligned}$$

where the chiral superfields are denoted as follows: S (singlet), H_1 and H_2 (Higgs doublets), T (antitop), B (antibottom), E (antitau), Q_3 (top-bottom doublet), L (tau-neutrino doublet). Let us briefly review the present status of these motivations for the (M+1)SSM.

A supersymmetric mass term $\mu H_1 \cdot H_2$ is added to the MSSM superpotential in order to avoid a potentially dangerous Peccei-Quinn symmetry and to allow for an acceptable minimum of the Higgs potential. The analysis of the $SU(2) \times U(1)$ breaking then requires μ to be roughly of the same order of magnitude as the soft terms that embody the supersymmetry breaking effects in the two Higgs sectors. This interesting hierarchy problem, the so-called μ -puzzle, has motivated many a suggestion to link the supersymmetric mass μ to supersymmetry breaking [9]. In any instance, some kind of new physics is requested and in this sense the MSSM that looks mostly economical at low energies is not necessarily so at the unification (GUT) level. A natural solution [10] is provided by the addition of a singlet S . Soft terms that break supersymmetry can induce a v.e.v. for S and an effective supersymmetric mass $\mu = \lambda S$ of the right order magnitude. This mechanism asks for the $\kappa S^3/3$ self-coupling in the superpotential which also breaks the unwanted Peccei-Quinn symmetry. However, this coupling would be forbidden and the singlet model inoperative if S has non-trivial quantum numbers with respect to broken symmetries beyond those of the Standard Model. This phenomenon is frequently found in superstring compactifications. We take here the pragmatic viewpoint that all the dimension three interactions that preserve the low-energy local and global symmetries are to be included. As we shall discuss later, very low values of the coupling κ are consistent with the phenomenological constraints. In this case, it could be a relic of non-renormalizable interactions after the decoupling of, *e.g.*, extra $U(1)$ gauge symmetries. Actually, the “sliding” singlet v.e.v. compensates for the smallness of the couplings κ and λ and this considerably reduces the fine-tuning problem of the μ -term. Such a possibility is indeed supported by our analysis.

Supersymmetric mass terms are forbidden by the \mathbb{Z}_3 symmetry of the purely cubic superpotential assumed in (1). This discrete symmetry also prevents S from getting a large v.e.v. through large radiative corrections to singlet tadpole terms, which invalidate other supersymmetric models with gauge singlets [11, 12]. On the other hand, the \mathbb{Z}_3 symmetry can give rise to cosmological problems in the form of domain walls which are produced during the electroweak phase transition [13]. Possible solutions to this problem have been discussed in [13] and include inflation of the weak scale, embedding of the discrete symmetry into a gauge symmetry at the Planck scale or re-introducing of the μ -term in the superpotential. (In the presence of the singlet, μ can be orders of magnitudes smaller than the weak scale, in which case our subsequent analysis is not affected; however, the μ -problem was part of the motivations of the model.) In any case, since we concentrate in this paper on the particle physics aspects of the model and do not discuss cosmological issues, our results will be independent of the form of the solutions of the domain wall problem.

The study of spontaneous CP breaking in the (M+1)SSM also differs

from the MSSM. Indeed, CP violating vacua can be induced only if there are more than one phase-dependent interaction in the scalar potential. In the MSSM, the only tree-level term is the soft scalar mass term $B\mu H_1 H_2$. Analytic terms of higher dimensions generated at the one loop level can conspire with the tree-level one to induce spontaneous CP violation. However, this has been shown [14] to entail a very low upper limit on one of the scalar masses which is inconsistent with present experiments at LEP. The classical scalar potential processes a richer structure in the (M+1)SSM, with three additional complex scalar couplings (one of dimension four, two cubic soft terms, see next section). The conditions for CP spontaneous breaking in this type of models have been shown [15] to imply a negative eigenvalue in the scalar (mass)² matrix. However, top quark-squark loop corrections could shift this eigenvalue to positive values. Thus spontaneous CP violation would occur for appropriate values of the parameters and one or two light scalars are predicted [16]. This issue certainly deserves a more detailed comparison with phenomenology; it lies outside the purview of the present investigation. Because the very small region in the (M+1)SSM parameter space consistent with spontaneous CP violation and those selected by our CP conserving solutions are apart, we disregard *ab initio* the question of non-trivial phase vacua.

Upper bounds have been derived for the mass of the lightest Higgs scalar in the MSSM that take into account the large one loop corrections [17] as well as some two-loop effects [18]. This prediction is of paramount importance in view of the experimental searches of the Higgs scalar in the LEP 200 and the LHC. The (M+1)SSM has an additional contribution $\propto |\lambda|^2$ to the Higgs (mass)². It has been shown [1, 3, 19] that requiring the theory to remain perturbative up to the GUT scale reduces this additional contribution to $< O(30 \text{ GeV})$. The upper bounds on the lightest Higgs boson mass are considerably lowered if one also imposes all phenomenological constraints needed for the model to be realistic. This has been done in the case of universal supergravity couplings [2, 3] and also for some special non-universal models [20]. Note that a relatively small increase in the Higgs mass may affect the experimental signatures. Since the predictions of the phenomenologically constrained (M+1)SSM for the Higgs sector has been the subject of a recent publication [5], we shall only give a short account of this important matter here.

As for the particle spectrum, this model presents several new features as compared to the MSSM. The supermultiplet S consists of two scalars of opposite CP and one Majorana fermion. After the $SU(2) \times U(1)$ breaking, these states get mixed with the neutral states in the Higgs doublet and gauge supermultiplets, leading to a slightly richer spectrum. In particular, since the visibility of physical states depends on their couplings to the gauge bosons and to matter, some particles could be relatively light if they are mainly gauge singlets. Thus, some of the limits on neutral particles obtained

at LEP in the MSSM framework do not immediately apply to the alternative (M+1)SSM. The discussion in this paper as well as in our previous ones [2, 5] is also aimed to persuade experimentalists to analyze their data on a more general basis.

In the $\kappa \rightarrow 0, \lambda \rightarrow 0$ limit, the gauge singlet decouples and the remaining theory looks like the MSSM [1]. However, this limit leads to a particular version of the MSSM with a strong correlation among the soft parameters, as we shall discuss later on. The singlet scalar takes a very large v.e.v. of $O(m_{3/2}/\kappa)$, but the fermion singlet and both scalar singlets are rather light.

Of course, the large dimension of the scalar field manifold allows for a rich structure in the overall scalar potential and leads to the existence of many local extrema [21]. One has to carefully check that the phenomenologically viable vacuum is favoured with respect to the unwanted ones. Among these there are the usual $SU(3)_c \times U(1)_{em}$ breaking ones, corresponding to vacua with quark and lepton quantum numbers [22], [21], [23]. In the (M+1)SSM there is the additional possibility of a non-vanishing charged Higgs field vacuum. However, the necessary condition for this particular charge violating classical solution is a relatively large coupling of the Higgses to the singlet [24], so that this situation is quite naturally avoided by a bound on that coupling. Our theoretical and experimental constraints turn out to automatically selected the right region of the parameter space.

Actually, as we shall discuss here below, an acceptable minimum of the potential requires some inequalities among the soft supersymmetry breaking terms which would tend to induce $SU(3)_c \times U(1)_{em}$ breaking vacua as well. The radiative corrections due to the gauge interactions then allow for a compromise while restricting the useful region in the parameter space. Since the electroweak gauge symmetry breaking is induced by radiative corrections involving the top Yukawa coupling – a well-known property in supersymmetric extensions of the Standard Model – the existence of a physically acceptable vacuum in the (M+1)SSM is a purely quantum effect.

3 Soft terms and boundary conditions

The supersymmetric part of the scalar potential is obtained from the superpotential through the well-known expression as a sum of F and D terms. The supersymmetry breaking part of the lagrangian contains all soft terms consistent with the symmetries of the superpotential: gaugino masses, trilinear analytic scalar couplings and scalar mass terms. In the (M+1)SSM they are as follows (with the same notation for the chiral matter supermultiplets and their first component complex scalars) :

$$\mathcal{L}_{\text{soft}} = (M_1\lambda_1\lambda_1 + M_2\lambda_2\lambda_2 + M_3\lambda_3\lambda_3 +$$

$$\begin{aligned}
& + A_\lambda \lambda S H_1 \cdot H_2 + A_\kappa \frac{\kappa}{3} S^3 + A_t h_t Q_3 \cdot H_2 T^c + h.c) + \\
& + m_1^2 |H_1|^2 + m_2^2 |H_2|^2 + m_S^2 |S|^2 + m_{Q_3}^2 |Q_3|^2 + m_T^2 |T^c|^2 + \\
& + \dots
\end{aligned} \tag{2}$$

where $\lambda_1, \lambda_2, \lambda_3$ are the gauginos associated to the $U(1)_Y, SU(2)$ and $SU(3)$ gauge symmetries. Only the terms involving the top scalars have been retained in (2), with $Q_3 = (T, B)$, but similar interactions for all other squarks and sleptons are to be understood. All the parameters are taken to be real (up to irrelevant phases) and flavour mixing is neglected. Notice that these soft terms contain all the dimensionful parameters of the model, which are all naturally related to the supersymmetry breaking scale M_{susy} . In order to study the particle spectrum and $SU(2) \times U(1)$ symmetry breaking in the (M+1)SSM, one should take the parameters in (1) and (2) at the relevant scales, the Fermi scale $v = 174$ GeV or M_{susy} . Instead, it is natural to fix these parameters at the level of the underlying supergravity theory. We shall consider here the unification scale $\Lambda_{\text{GUT}} \sim 10^{16}$ GeV to define them. This is just a few orders of magnitude below the Planck mass and one can presumably assume an effective renormalizable theory at Λ_{GUT} . Once the parameters are given at Λ_{GUT} , their corresponding values at v or M_{susy} are calculated by the integration of the renormalization group equations (RGE) for the (M+1)SSM [21]. We present in the appendix the analytic solutions of the (M+1)SSM RGE in the approximation $h_i^2 \gg \lambda^2, \kappa^2$, which turns out to be good for most of the set of parameters that will be selected on a phenomenological basis. However, for the sake of precision, we numerically integrate the RGE in our analysis, the expressions in the Appendix being reserved for analytical discussions of the numerical results. In practice, we renormalize the parameters down to the scale v through the supersymmetric RGE, and then apply the Coleman-Weinberg corrections to the Higgs potential to take into account the decoupling of the stops at M_{susy} .

The important hypothesis to be made in this paper is the so-called ‘‘universality’’ or flavour-independence for the soft-terms in (2). For the supersymmetry breaking scalar interactions it amounts to assume a common value for all the parameters A_i in (2) (at Λ_{GUT}),

$$A_\lambda = A_\kappa = A_t = A_b = A_\tau = \dots = A_0, \tag{3}$$

and the same values (at Λ_{GUT}) for the scalar masses in (2),

$$m_1^2 = m_2^2 = m_S^2 = m_{Q_3}^2 = m_T^2 = \dots = m_0^2. \tag{4}$$

This universality follows if the direction of supersymmetry breaking, characterized by the goldstino components, corresponds to fields with purely gravitational couplings to the relevant chiral superfields (for instance, if it is along the dilaton-axion direction in superstring inspired theories [26]). Of

course, it follows in general if the goldstino components have equal couplings to all relevant chiral superfields; an example is given by the “large radius limits” of orbifold compactifications in string theory if supersymmetry breaking occur along the modulus direction [27].

As for gaugino masses, the universality hypothesis at Λ_{GUT} reads

$$M_1(\Lambda_{\text{GUT}}) = M_2(\Lambda_{\text{GUT}}) = M_3(\Lambda_{\text{GUT}}) = M_0. \quad (5)$$

In grand unified gauge theories many of these relations will be required by the enlarged gauge group at the tree-level. At the one loop level one expects some threshold corrections to the universality of the soft terms already at the reference scale Λ_{GUT} . The deviations from (3) - (5) in the matter sector can be phenomenologically important because of the existent experimental bounds on FCNC effects but they are less relevant to our discussion in this paper.

Deviations from the universality assumption are also possible in the framework of superstring theory, since the moduli sector can couple differently to the various chiral fields. Since the assumptions $A_\kappa(\Lambda_{\text{GUT}}) = A_\tau(\Lambda_{\text{GUT}})$ and $m_1^2(\Lambda_{\text{GUT}}) = m_2^2(\Lambda_{\text{GUT}}) = m_S^2(\Lambda_{\text{GUT}}) = m_E^2(\Lambda_{\text{GUT}}) = m_L^2(\Lambda_{\text{GUT}})$ play an important role in our phenomenological analysis, some of our results depend on the universality of the supersymmetry breaking parameters. However a similar analysis of the (M+1)SSM has been published [20] for the case of non-universal soft terms in the framework of an orbifold compactification of the superstring, and these results are quite analogous to those presented here.

The most important consequences of the flavour independence of soft terms concern the $SU(2) \times U(1)$ symmetry breaking. It could be induced by a negative value of m_2^2 , but for the potential to be bounded from below and to avoid colour or *e.m.* symmetry breaking the universal parameter m_0^2 has to be positive, so that $m_2^2(\Lambda_{\text{GUT}}) > 0$. For this reason, $m_2^2(v) < 0$ has to be enforced by renormalization effects. This is a well-known feature of the MSSM as well, entailing a lower limit on the top Yukawa coupling. In the (M+1)SSM, the sign of m_2^2 could be made to flip by the coupling of the singlet fields even for a light top quark [21]. The experimental value of top quark mass is perfectly consistent, however, with a negative m_2^2 at low energies from the effects of top-stop quantum loops.

Furthermore the cubic soft terms can also induce spontaneous symmetry breaking if the value of the parameter A in (3) is large enough. Hence large values of A_κ are preferred to give the singlet scalar a v.e.v.. However, with the universality assumption (3), the squark and sleptons could also get non-vanishing v.e.v.’s [22, 21, 23]. Interestingly enough, the gauge interactions reduce the A -parameters for matter fields while preserving the value of A_κ , as can be seen from the expressions in the Appendix. Thus, phenomenologically consistent (M+1)SSM’s with the condition (3),(4),(5), can

be build at the price of restricting the space of the supersymmetry breaking parameters. This is the most important restriction imposed on the model by the universality hypothesis, as compared to the MSSM [2]. Otherwise, the effects of this universality on the $SU(2) \times U(1)$ spontaneous breaking are similar to those in the MSSM.

Another consequence of this assumption is to reduce the number of free bare parameters in the (M+1)SSM to five (before imposing the physical constraints) just like in the MSSM: the dimensionful parameters B and μ of the latter are replaced in the former by the dimensionless parameters λ and κ .

At low energies, the soft terms as obtained from the RGE depend on the parameters M_0, A_0, m_0^2 , on the choice of the GUT scale, Λ_{GUT} , through $t = \ln(\Lambda_{\text{GUT}}/v) / (16\pi^2)$ (a typical value being $t \simeq .21$), and on the gauge and Yukawa couplings. This calculation has to be done numerically in general. However, from the dimensionality of these running parameters, they can be generically expressed at low energy in terms of their universal initial values as

$$\begin{aligned} A_i(t) &= a_i A_0 + b_i M_0 \\ m_i^2(t) &= z_i m_0^2 + x_i A_0^2 + y_i A_0 M_0 + w_i M_0^2 \end{aligned} \quad (6)$$

where the coefficients depend on the various gauge and Yukawa couplings. For the simple case where the top Yukawa coupling dominates over the others, the dependence on the latter reduces to simple expressions in terms of the ratio $\rho = h_t^2(v)/h_{\text{crit}}^2$ where $h_{\text{crit}} \simeq 1.1$ is the fixed point value of the top Yukawa coupling. The results of this approximation are presented in the Appendix and are used for the sake of some qualitative understanding of the numerical results. With the recent measurements of the top quark mass, ρ is bounded by $\rho \gtrsim 2/3$ (this is higher than the minimum value required to induce mediative $SU(2) \times U(1)$ breaking). As an example, we list the low energy soft parameters at the fixed point value $\rho = 1$. The coefficients are approximated to a reasonable precision.

$$\begin{aligned} A_\kappa &\simeq A_0 & A_\lambda &\simeq \frac{1}{2}(A_0 - M_0) & A_t &\simeq 2M_0 \\ m_1^2 &\simeq m_0^2 + \frac{1}{2}M_0^2 & m_2^2 &\simeq -\frac{m_0^2}{2} - 3M_0^2 & m_S^2 &\simeq m_0^2 \\ m_T^2 &\simeq 4M_0^2 & m_{Q_3}^2 &\simeq \frac{1}{2}m_0^2 + 6M_0^2 \end{aligned} \quad (7)$$

4 Mass spectrum in the Higgs sector and vacuum structure

Let us first restrict the discussion to the physically relevant vacua with (real) v.e.v.'s for the field $\langle H_2^0 \rangle = h_2, \langle H_1^0 \rangle = h_1, \langle S \rangle = s$. The scalar potential restricted to this sector reads ($\bar{g}^2 = g_1^2 + g_2^2$)

$$\begin{aligned}
 V = & (\kappa S^2 + \lambda H_1^0 H_2^0)^2 + \lambda^2 |S|^2 (|H_1^0|^2 + |H_2^0|^2) + \\
 & + \left(A_\lambda \lambda S H_1^0 H_2^0 + A \kappa \frac{\kappa}{3} S^3 + h.c. \right) + m_1 |H_1^0|^2 + m_2^2 |H_2^0|^2 + \\
 & + m_S^2 |S|^2 + \frac{\bar{g}^2}{4} (|H_1^0|^2 - |H_2^0|^2)^2 + V_{\text{rad}}
 \end{aligned} \tag{8}$$

where V_{rad} is the quantum correction to the effective scalar potential beyond the RGE effects included in the running parameters of (8). These radiative corrections are important, in particular in the evaluation of the lightest Higgs boson mass. The relevant contribution comes from the top-stop sector because of the relatively large value of the top Yukawa coupling. Hence we only include the top quark and the two stop states, T_1 and T_2 in the usual Coleman-Weinberg expression,

$$V_{\text{rad}} = \frac{1}{64\pi^2} \text{STr } m^4 \ln \frac{m^2}{Q^2} \tag{9}$$

The appropriate mass terms in (9) are then the top quark mass m_t^2 and the stop masses

$$\begin{aligned}
 m_{T_{1,2}}^2 &= m_t^2 + \frac{1}{2} (m_{Q_3}^2 + m_T^2) \pm W, \text{ where} \\
 W^2 &= \frac{1}{4} (m_{Q_3}^2 + m_T^2) + h_t^2 |A_t h_2 + \lambda s h_1|^2, \\
 m_t &= h_t h_2.
 \end{aligned} \tag{10}$$

All the parameters in (8) and (9) are to be taken at the scale $Q^2 \sim O(h_1^2 + h_2^2)$.

These radiative corrections are mostly due to the splitting between the quarks and the squarks. However, even if one starts from universal parameters at Λ_{GUT} , the RGE running introduce some asymmetry in the stop sector as can be seen from the formulae in the Appendix. The resulting splitting in $m_{T_1}^2 - m_{T_2}^2$ produces a sizeable effect in V_{rad} and in the scalar mass spectrum. The full one loop expressions for the mass matrices and the potential minimization are available in the literature. All the numerical calculations in the present paper are performed by using the formulae in [8]. However, for the sake of the analytic approximations discussed below we use

a simple approximation by keeping only the lowest relevant order in the development in terms of the stop splitting, $(m_{T_1}^2 - m_{T_2}^2) / (m_{T_1}^2 + m_{T_2}^2)$. The minimization of the scalar potential amounts to the following conditions

$$\begin{aligned}
h_1 \left[m_1^2 + \hat{\mu}^2 \left(1 + \frac{h_2^2}{s^2} \right) + \frac{1}{2} \bar{g}^2 (h_1^2 - h_2^2) + \right. \\
\left. + \hat{B} \hat{\mu} \frac{h_2}{h_1} + \beta_t \hat{\mu}^2 L \right] &= 0 \\
h_2 \left[m_2^2 + \hat{\mu}^2 \left(1 + \frac{h_1^2}{s^2} \right) - \frac{1}{2} \bar{g}^2 (h_1^2 - h_2^2) \right] + \\
+ \hat{B} \hat{\mu} \frac{h_1}{h_2} + \beta_t \left[\left(m_T^2 + m_{Q_3}^2 + A_t^2 \right) (L + \varepsilon) \right. \\
\left. - \left(m_T^2 + m_{Q_3}^2 \right) + 2m_t^2 L \right] &= 0 \\
s \left[m_S^2 + \hat{\mu} \frac{h_1^2 + h_2^2}{s^2} + 2\nu^2 + A_\kappa \nu + \left(\hat{B} + \nu \right) \hat{\mu} \frac{h_1 h_2}{s^2} + \right. \\
\left. + \beta_t \hat{\mu}^2 \left(\frac{h_2}{s} \right)^2 (L + \varepsilon) \right] &= 0
\end{aligned} \tag{11}$$

where

$$\beta_t = \frac{3h_t^2}{16\pi^2}, \quad \varepsilon = \ln \frac{m_t^2}{Q^2}, \quad L = \ln \frac{m_{T_1} m_{T_2}}{m_t^2} \tag{12}$$

and the variables

$$\begin{aligned}
\hat{\mu} &= \lambda s \\
\nu &= \kappa s \\
\hat{B} &= A_\lambda + \nu + \beta_t A_t (L + \varepsilon)
\end{aligned} \tag{13}$$

have been introduced. An one loop term has been conveniently included in the definition of the effective parameter \hat{B} (of the MSSM).

The 3×3 mass matrix for the CP even scalars (in the same approximation) has the following matrix elements

$$\begin{aligned}
m_{11}^2 &= \bar{g}^2 h_1^2 - \hat{B} \hat{\mu} \left(\frac{h_2}{h_1} \right) - \beta_t \hat{\mu}^2 \frac{Z^2}{3} \\
m_{22}^2 &= \bar{g}^2 h_2^2 - \hat{B} \hat{\mu} \left(\frac{h_1}{h_2} \right) + 4\beta_t m_t^2 L + \beta_t A_t \left(2m_t Z - A_t \frac{Z^2}{3} \right) \\
m_{SS}^2 &= (A_\kappa + 4\nu) \nu - \left(\hat{B} - \nu \right) \hat{\mu} \frac{h_1 h_2}{s^2} - \frac{\hat{\mu}^2}{3} \left(\frac{h_1^2}{s^2} \right) \beta_t Z^2
\end{aligned}$$

$$\begin{aligned}
m_{1S}^2 &= 2\hat{\mu}^2 \left(\frac{h_1}{s}\right) + (\hat{B} + \nu) \hat{\mu} \left(\frac{h_2}{s}\right) + \beta_t \hat{\mu}^2 \left(\frac{h_1}{s}\right) \left(L + \varepsilon - \frac{1}{2}\right) \\
m_{2S}^2 &= 2\hat{\mu}^2 \left(\frac{h_2}{s}\right) + (\hat{B} + \nu) \hat{\mu} \left(\frac{h_1}{s}\right) + \hat{\mu} \left(\frac{h_1}{s}\right) \beta_t \left(m_t Z - A_t \frac{Z^2}{3}\right) \\
m_{12}^2 &= -\bar{g}^2 h_1 h_2 + 2\hat{\mu}^2 \left(\frac{h_1 h_2}{s^2}\right) + \hat{B} \hat{\mu} + \hat{\mu} \beta_t \left(m_t Z - A_t \frac{Z^2}{3}\right) \\
Z &= \frac{m_t (A_t + \hat{\mu} \cot \beta)}{m_t^2 + \frac{1}{2} (m_{Q_3}^2 + m_T^2)} \tag{14}
\end{aligned}$$

The parameter L characterizes the top-stop mass splitting and can be relatively large, while ε depends on the low energy scale chosen to define the running parameters — we take $Q^2 \sim (h_1^2 + h_2^2)$ in this paper so that $|\varepsilon| \sim |\ln h_t^2| < 1$.

The CP odd scalar (mass)² matrix with the would-be Goldstone boson projected out is as follows,

$$\begin{pmatrix} -\hat{B} \hat{\mu} \frac{h_1^2 + h_2^2}{h_1 h_2} & -(\hat{B} - 3\nu) \hat{\mu} \frac{\sqrt{h_1^2 + h_2^2}}{s} \\ -(\hat{B} - 3\nu) \hat{\mu} \frac{\sqrt{h_1^2 + h_2^2}}{s} & -3A_\kappa \nu - (\hat{B} + 3\nu) \hat{\mu} \frac{h_1 h_2}{s^2} \end{pmatrix} \tag{15}$$

The minimization of the potential fixes $\hat{B} \hat{\mu}$ and $A_\kappa \nu$ to be negative, so that the diagonal entries in (15) are positive. The (mass)² of the charged scalar reads

$$m_{H^+}^2 = M_W^2 \left(1 - \frac{\lambda^2}{g_2^2}\right) + \left| \hat{B} \hat{\mu} \frac{h_1^2 + h_2^2}{h_1 h_2} \right| \tag{16}$$

The radiative corrections are incorporated into the CP odd neutral and charged scalar masses through the shift of the \hat{B} parameter as defined in (13) [8].

Although all the numerical results in this paper are obtained by numerical minimization of the complete one loop potential (8), (9) and the numerical determination of the mass eigenvalues, it is interesting to get some insight into the results through simple analytic approximations. Indeed, many features of the particle spectrum of the (M+1)SSM are related to an important property, first noticed in [2], namely: the only physically acceptable solutions of the vacuum equations (11) are large singlet solutions: $s \gtrsim 1\text{TeV} \gg h_2, h_1$. Indeed, solutions with $s \lesssim h_2$ lead to one or more light states in the spectrum that are excluded by experiments, specially by LEP experiments. Examples can be found in [1], where the parameters have been chosen to yield light spectrum. The general character of this feature of the (M+1)SSM has been carefully checked in our numerical analysis. Having settled this fact one can go on to establish several approximate consequences.

(A) The S v.e.v is approximately obtained from the third equation in (11) with $h_2 = h_1 = 0$,

$$s \simeq \frac{-A_\kappa - \sqrt{A_\kappa^2 - 8m_S^2}}{4\kappa} \quad (17)$$

The potential at this value of s has also to be negative in the allowed region of the parameter space, as discussed in more detail in section 5. This additional condition requires

$$9m_S^2 < A_\kappa^2 \quad (18)$$

This approximation turns out to be very accurate. The parameters A_κ and m_S^2 are only slightly renormalized if $\kappa, \lambda \ll 1$. Actually, these relatively low values of the couplings are also required by our numerical study of the model, so that the condition (18) approximately applies to the bare universal parameters A_0, m_0^2 , yielding the strong constraint in the parameter space:

$$A_0^2 \gtrsim 9m_0^2 \quad (19)$$

The S v.e.v. in (17) defines the effective parameters \hat{B} and $\hat{\mu}$ analogous to those often denoted B and μ in the MSSM. Indeed, up to corrections of $O(h_2^2/s^2)$, the first two equations in (11) are the same as in the MSSM with the introduction of these parameters. Notice that $\hat{\mu} \sim \lambda A_\kappa / 2\kappa$ should be of $O(m_{3/2})$. Hence the well-known ‘‘fine-tuning’’ on the MSSM free parameter, $\mu \sim O(m_{3/2})$, is replaced here by the requirement of no strong hierarchy between the λ and κ Yukawa couplings, as the $SU(2) \times U(1)$ invariant scale of the singlet field is dynamically fixed by supersymmetry breaking, accordingly to (17).

With $\tan \beta = h_2/h_1$ one recovers, in this approximation, the MSSM relation

$$\tan^2 \beta = \frac{m_1^2 + \beta_t \hat{\mu}^2 L + \hat{\mu}^2 + M_Z^2/2}{m_2^2 + (m_{T_1}^2 + m_{T_2}^2 + A_t^2) \beta_t L + \hat{\mu}^2 + M_Z^2/2} \quad (20)$$

Only the dominant terms of the radiative corrections are retained. Because the denominator in (20) has terms of either sign ($m_2^2 < 0$) it is relatively sensitive to radiative corrections which tend to decrease $\tan \beta$ with respect to the tree-level approximation.

(B) In the neutral scalar mass matrices (14,15) as well as in the neutralino mass matrices, the mixing of the singlet fields to the others is always proportional to h_1/s and h_2/s , hence small. This is the reason why, in most of the allowed points of the parameter space, the singlet sector of the theory, after dynamically producing the effective parameters (13), is almost decoupled from the rest of the theory that resembles to the MSSM.

(C) The MSSM is formally obtained in the limit $s \rightarrow \infty$ with ν and $\hat{\mu}$ fixed ($\kappa, \lambda \ll \bar{g}^2$). In this limit the singlet sector decouples from the doublet Higgs sector, and the singlet masses are:

$$\begin{aligned}
& \frac{1}{4} \sqrt{A_0^2 - 8m_0^2} \left(|A_0| + \sqrt{A_0^2 - 8m_0^2} \right) \text{ (CP even scalar)} \\
& \frac{3}{4} |A_0| \left(|A_0| + \sqrt{A_0^2 - 8m_0^2} \right) \text{ (CP odd scalar)} \\
& \left(|A_0| + \sqrt{A_0^2 - 8m_0^2} \right) / 2 \text{ (singlet fermion, singlino)}.
\end{aligned} \tag{21}$$

The singlet particles become light in the small A_0 limit. We argue in section 5 that this limit is always associated to the singlet decoupling limit ($\kappa \rightarrow 0, s^2 \gg h_1^2 + h_2^2$). Some of the physical consequences of a light singlino are discussed in section 6.

The neutral and charged Higgs² sector, as well as other neutralinos and charginos follow the MSSM pattern. In this sense the (M+1)SSM reduces to the MSSM in this limit but with an important restriction in the parameter space needed to dynamically implement the physically acceptable vacuum.

5 Constraints on the parameter space from vacuum stability

The spontaneous breaking of $SU(2) \times U(1)$ symmetry in the (M+1)SSM restricts even more the (M_0, m_0^2, A_0) parameter subspace than in the MSSM under the same assumption of universality. The minimum discussed in section 3 has to be cosmologically flavourless and stable with respect to other possible minima. The first constraint comes from the fact that the S v.e.v. is induced through the “ A -mechanism” [26, 10] with $A_0^2 > 9m_0^2$, as given in (19). It is well known that large A_0 values may induce charged and coloured vacua.

In order to avoid slepton v.e.v.’s one has to impose

$$A_e^2 < 3(m_E^2 + m_L^2 + m_1^2) \tag{22}$$

²As can be seen from (16) there is a negative contribution $\lambda^2 M_Z^2 / \bar{g}^2$, to $m_{H^+}^2$. This is the origin of the condition $\lambda^2 < \bar{g}^2$ which is sufficient to avoid *e.m.* charge breaking through $\langle H^+ \rangle \neq 0$, which is satisfied anyway by the models that are consistent with the other phenomenological constraints.

at a scale $\Lambda \lesssim 0(A_e/h_e)$, where (A_e/h_e) characterizes the scale of the would-be slepton *v.e.v.'s*. From the RGE solutions in the appendix this implies $(t_e = \ln(h_e \Lambda_{\text{GUT}}/A_e)/16\pi^2)$,

$$\begin{aligned} & (A_0 + 2M_0 t_e (3g_2^2 + 3g_1^2)) \\ < & 9 [m_0^2 + 2g_2^2 t_e (1 - g_2^2 t_e) M_0^2 + 2g_1^2 t_e (1 - 11g_1^2 t_e) M_0^2]. \end{aligned} \quad (23)$$

The most dangerous v.e.v.'s comes from the electron sector with the smallest Yukawa and the largest scale $A_e/h_e \sim 0(10^8 \text{ GeV})$, and (22) at this scale finally becomes

$$(A_0 + .4M_0)^2 < 9m_0^2 + 2.4M_0^2. \quad (24)$$

This can be combined with the condition $A_0^2 > 9m_0^2$ to obtain restrictions on the ratio A_0/M_0 . For this purpose we introduce a parameter to characterize the fine-tuning of m_0^2 with respect to A_0 ,

$$\alpha = \frac{A_0^2 - 9m_0^2}{A_0^2} \quad (25)$$

and obtain from (24) the upper bound on α

$$\left| \frac{M_0}{A_0} \right| > .18 (\sqrt{14\alpha + 1} + \text{sign}(A_0/M_0)) \quad (26)$$

For $A_0/M_0 > 0$, (24) yields the limit

$$M_0^2 > \frac{A_0^2}{8} > m_0^2 \quad (27)$$

For $A_0/M_0 < 0$, $|A_0|$ can become much larger than M_0 at the price of a fine-tuning of m_0^2/A_0^2 corresponding to α of $O(M_0/A_0)$. Though these conditions are only valid under the universality assumption for soft terms, analogous ones can be derived along the same lines for other models (see, *e.g.*, [20]). (Strictly speaking, (24) can only be analytically derived [21] if the scalars are relatively degenerate. But recent numerical studies suggest that it is approximately valid under more general conditions [25])

The next step is to avoid minima with $\langle H_1 \rangle = 0$, i.e., with $\tan \beta \rightarrow \infty$. In this analysis the radiative corrections discussed in section 3 can be relevant. Of course, in our numerical analysis they are included, but in order to understand the origin of some of the constraints on the (M+1)SSM parameter space, they are neglected in some of the expressions here below. In the effective two-step minimization of the scalar potential, one finds for the phenomenologically acceptable solution discussed in the previous section the approximate value at the minimum

$$\begin{aligned}
V_{\min} &= \frac{-A_\kappa^4}{48\kappa^2} C(\alpha) - \frac{M_Z^4}{4\bar{g}^2} \cos^2 2\beta \\
C(\alpha) &= \left(\frac{3 + \sqrt{1 + 8\alpha}}{6} \right)^3 \left(\frac{\sqrt{1 + 8\alpha} - 1}{2} \right)
\end{aligned} \tag{28}$$

where the first term comes from the pure singlet sector and the last one from the effective MSSM potential defined with the parameters given by (13). This physical minimum has to be compared with another one, with $\langle S \rangle = \langle H_1 \rangle = 0$ and $\langle H_2^2 \rangle = -m_2^2/2\bar{g}^2$. The potential at this minimum is

$$V'_{\min} = -\frac{(m_2^2)^2}{\bar{g}^2} \tag{29}$$

In principle one should look for the cosmological formation and stability of the minimum (28) with respect to (29). For simplicity we replace the rigorous constraints by the simpler condition that $V_{\min} < V'_{\min}$, *i.e.*, that the absolute minimum is the physical one. This stability condition differs from the corresponding one within the MSSM in two respects: (i) the presence of the pure singlet negative term in (28) favours V_{\min} ; (ii) in the MSSM, $(-m_2^2)^2$ is replaced by $(-m_2^2 + \hat{\mu}^2)^2$ in (29), so that V'_{\min} is more dangerous in the (M+1)SSM. The comparison of (28) and (29) leads to the condition (at the scale v),

$$\frac{\bar{g}^2 A_\kappa^4}{48\kappa^2} C(\alpha) + \frac{M_Z^4}{4} \cos^2 2\beta > (m_2^2)^2. \tag{30}$$

On the other hand, from the RGE solution in the appendix one gets

$$-m_2^2 > \left(\frac{3\rho}{2} - 1 \right) m_0^2 + \left(4\rho - \frac{1}{2} \right) M_0^2 \tag{31}$$

and the measured values of the top mass does not allow for small $\rho = h_t^2/h_{\text{crit}}^2$ so that $\rho \gtrsim 2/3$. In addition, in the next section we derive from the experimental limits on the chargino masses a bound on M_Z/M_0 ,

$$\frac{2M_0}{\sqrt{5}} > M_Z = \bar{g} \sqrt{h_1^2 + h_2^2}. \tag{32}$$

(At this point, one is introducing experimental information on the spectrum. As already stressed, it is the interplay between the LEP bounds on sparticle masses and the vacuum conditions that constrains the parameter space.) Now, from (32) and (31), (30) can be well approximated by

$$\frac{\bar{g}}{4\sqrt{3}\kappa} > \left(\frac{M_0^2}{A_0^2} \right) \frac{(4\rho - \frac{1}{2})}{\sqrt{C(\alpha)}} \tag{33}$$

Notice that the necessary condition $C(\alpha) > 0$, which follows from (32) and (30), implies $\alpha > 0$, namely, the condition (19).

For $A_0/M_0 > 0$ one obtains from (26) and (33) the bound

$$\frac{\kappa}{\bar{g}} < \frac{1}{5(4\rho - \frac{1}{2})}, \quad (34)$$

so that κ is always relatively small, $\kappa < \bar{g}/10 = 0.05$. This is related to the large values taken by the S v.e.v.. Indeed by replacing (17) and (32) in (33), we obtain

$$\frac{|s|}{\sqrt{h_1^2 + h_2^2}} > \sqrt{3}(8\rho - 1) > 7. \quad (35)$$

Of course, the limits (34) and (35) are relatively loose bounds and most of the solutions of our numerical studies correspond to smaller (larger) values of κ (s , respectively). Also to be noticed is the behaviour of s for fine-tuning of the parameter α in (25): $s/\sqrt{h_1^2 + h_2^2} \rightarrow (4\rho - 1/2)/\sqrt{\alpha}$ as $\alpha \rightarrow 0$, while κ decreases as $\sqrt{\alpha}$.

For $A_0/M_0 < 0$, the situation is more involved since one can allow for large values of A_0 with some fine-tuning of the m_0^2/A_0^2 ratio. The relations corresponding to (34) and (35) are respectively

$$\begin{aligned} \frac{\kappa}{\bar{g}} &< \frac{1}{2(4\rho - \frac{1}{2})} \frac{1}{\sqrt{\alpha}} \left(1 + \frac{1}{6\alpha}\right) \\ \frac{|s|}{\sqrt{h_1^2 + h_2^2}} &> \left(2\rho - \frac{1}{4}\right) \frac{7\sqrt{\alpha}}{(1 + \alpha)} \end{aligned} \quad (36)$$

For moderate values of α , (36) corroborate our conclusions from (34) and (35). In the fine-tuning limit, $\alpha \rightarrow 0$, the singular behaviour of κ in the parameter α is apparent. However, in this case our approximations are not powerful enough to explain the lower bound [2] $s \gtrsim 6\sqrt{h_1^2 + h_2^2}$ that is found in our numerical analysis.

Another interesting constraint follows from (20) which implies $-(m_2^2 + (m_{T_1}^2 + m_{T_2}^2 + A_t^2) \beta_t L) < \hat{\mu}^2 + M_Z^2/2$. Neglecting the top-stop radiative corrections and using (31) and (32) yields,

$$\hat{\mu}^2 = \lambda^2 s^2 > (4\rho - 1) M_0^2 \quad (37)$$

From (17) and (26), one derives the limits:

$$\begin{aligned} (\lambda^2/\kappa^2) &> (4\rho - 1) \quad (A_0/M_0 > 0) \\ &> (4\rho - 1)(3\alpha/(1 + 2\alpha)) \quad (A_0/M_0 < 0) \end{aligned} \quad (38)$$

For moderate values of α this implies $\kappa^2 < \lambda^2$. At the price of some fine-tuning and $A_0/M_0 < 0$ one can obtain κ slightly larger than λ .

Concerning the important parameter $\tan \beta$, some simple qualitative predictions can be obtained from the following expression,

$$\frac{-2\hat{B}\hat{\mu}}{m_1^2 + m_2^2 + \left(m_{T_1}^2 + m_{T_2}^2 + A_t^2 + \hat{\mu}^2\right) \beta_t L + 2\mu^2} = \sin 2\beta \quad (39)$$

which is equivalent to (20) by the minimum conditions (11). Notice that $\text{sign}(\tan \beta) = -\text{sign}(\hat{B}\hat{\mu})$. From the renormalized expression (55) in the appendix, one sees that for $A_0 M_0 < 0$ the sign of \hat{B} is preserved and its magnitude increased by the gauge renormalisation proportional to M_0 which increases the numerator in (39). Therefore, in this case, $\tan \beta > 0$ and it can take relatively small values for $|A_0| > |M_0|$. Instead, for $A_0 M_0 > 0$, where (27) also applies, the M_0 term in (55) tends to exceed the A_0 term so that in most cases $\tan \beta < 0$ and its magnitude is relatively large. (Exceptions are the special cases with small ρ and $|A_0| \gtrsim 2|M_0|$ with a positive large $\tan \beta$.)

Therefore, with these simple analytic approximations for the vacuum conditions, together with the approximated condition from the experimental limits on the gauginos (to be discussed later on), one easily understands the qualitative pattern of the allowed parameter space as obtained from the detailed numerical investigation. For instance, (35) and (36) are related to the decoupling of the singlet sector, whereas sizeable mixing - which requires $s/\sqrt{h_1^2 + h_2^2} \sim O(1)$ - is possible only with the fine-tuning (and signs) discussed below (36).

6 Qualitative aspects of the mass spectrum

Let us first consider the chargino masses given by the expression

$$\begin{aligned} m_{\chi^\pm}^2 &= \frac{1}{2} (M_2^2 + \hat{\mu}^2 + M_W^2) \\ &\pm \frac{1}{2} \sqrt{(M_2^2 + \hat{\mu}^2 + M_W^2)^2 - (2\hat{\mu}M_2 - M_W^2 \sin 2\beta)^2} \end{aligned} \quad (40)$$

with $M_2^2/M_0^2 \simeq 2/3$. For the LEP experimental limit we take $m_{\chi^\pm} > 65$ GeV. Of course, the constraints from this limit on the parameters are the same as in the MSSM (with $\tan \beta$ in the more restricted range determined by the (M+1)SSM as discussed in section 8). On the other hand, this constraint plays an important role in the discussion of the previous section as well as in this section.

Because the scale of the soft supersymmetry breaking parameters is set by the weak scale, we conveniently express the dimensionful parameters in

terms of M_Z in this section. One can use the experimental bound, together with (20) and the (31), to deduce the relations

$$\hat{\mu}^2 > \left(6\rho - \frac{3}{4}\right) M_2^2 - \frac{M_Z^2}{2} > M_2^2 > m_{\chi^+}^2 > M_Z^2/2. \quad (41)$$

Let us now define a parameter a by,

$$\hat{\mu}^2 + \frac{M_Z^2}{2} = (a - 1) M_2^2 \quad (42)$$

which, for $\tan \beta \gtrsim 2$ (which turns out to be always the case in our numerical analysis), satisfies the approximate inequalities $6\rho + 1/4 \lesssim a \lesssim 6\rho + 2$. Then, from (40) and (41) one gets the following expression for the lightest chargino mass,

$$m_{\chi^+}^2 \simeq \frac{(a - 1)}{a} M_2^2 - \left(1 + \frac{2\sqrt{a}}{\tan \beta}\right) \frac{3M_Z^2}{4a}, \quad (43)$$

so that the approximate bounds,

$$\frac{1}{14} M_3^2 - \frac{1}{2} M_Z^2 \simeq \frac{3}{4} M_2^2 - \frac{1}{3} M_Z^2 \lesssim m_{\chi^+}^2 \lesssim \frac{7}{8} M_2^2 - \frac{1}{6} M_Z^2 \simeq \frac{2}{25} M_3^2 - \frac{1}{6} M_Z^2 \quad (44)$$

are obtained by varying the parameters ρ and $\tan \beta$, and by using the relation between the gluino and wino masses $M_3^2/M_2^2 \simeq 10.7$. This defines a relatively narrow band for m_{χ^+} as a function of the gluino mass M_3 , that is reasonably reproduced in our numerical analysis. It just expresses the fact that the lightest chargino is mostly a wino, with a component of $O(1/a)$ of the higgsino.

Now, from (44) and the experimental LEP bound, $m_{\chi^+}^2 > M_Z^2/2$, one gets a limit on the gluino mass, $M_3 \gtrsim 3M_Z = 273$ GeV (from the previous LEP bound, $m_{\chi^+} > M_Z/2$, the corresponding result was $M_3 \gtrsim 180$ GeV, but needed a more detailed approximation than (44)). This corresponds to $M_0 \gtrsim 100$ GeV. Notice that these are only approximations aimed to explain rather than predict the numerical results that take all the parameters into account. As already stressed, this result is analogous to the limits on the chargino masses in the MSSM. For $M_0 \gg M_Z$ the off-diagonal terms become relatively unimportant and $\hat{\mu}^2 \rightarrow (a - 1)M_2^2$. Therefore the lightest chargino is mostly a wino with $m_{\chi_1^+} \simeq M_2$ and the other chargino has mass $m_{\chi_2^+} \simeq \sqrt{a - 1}m_{\chi_1^+} > \sqrt{3}m_{\chi_1^+}$.

We next consider the neutralino sector, with five Majorana fermions. It is particularly important since it includes the lightest odd R-parity state, or LSP, and since its phenomenology can deviate from that predicted in the MSSM because of the presence of the singlet fermion (singlino, \tilde{s}). The mass terms for the neutralinos are,

$$\begin{aligned} & \tilde{s} \left[2\nu\tilde{s} + \frac{\lambda}{\tilde{g}} M_Z \left(\tilde{h}_1 \sin \beta + \tilde{h}_2 \cos \beta \right) \right] + \hat{\mu} \tilde{h}_1 \tilde{h}_2 + M_1 \tilde{B} \tilde{B} + M_2 \tilde{W}_3 \tilde{W}_3 \\ & + M_Z \left(\tilde{B} \sin \theta_w + \tilde{W}_3 \cos \theta_w \right) \left(\tilde{h}_1 \cos \beta + \tilde{h}_2 \sin \beta \right) \end{aligned} \quad (45)$$

The point to be stressed is the relatively small mixing of the singlino to the higgsinos. This is because $s \gg h_2 > h_1$ and $(2/3)|A_0| < |12\nu| < |A_0|$, $\hat{\mu} = \lambda s \gtrsim \sqrt{2}M_0 > \sqrt{2}M_Z$. Hence the singlino remains an almost pure state of mass $|2\nu|$, and the higgsino-gaugino sector is analogous to the charged one. The experimental constraints on the chargino imply, as just discussed, that the lightest chargino is mostly a gaugino, which will also imply an analogous situation in the non-singlet neutralino sector.

One finds indeed that the lightest states are ³: one which is mostly \tilde{B} , with a mass $\simeq M_1 \simeq M_0/\sqrt{6}$, and another one, mostly \tilde{W}_3 , with mass $\simeq M_2 \simeq 2M_1$. From the bound on the chargino mass one has $M_1^2 > M_Z^2/5$. The most important difference between the (M+1)SSM and the MSSM could be in the LSP character: unless one badly violates the universality assumption for the scalar masses, the LSP is mostly a \tilde{B} in the MSSM, while the \tilde{s} is also a LSP candidate in the (M+1)SSM. Let us consider the condition for a *singlino* LSP,

$$|2\nu| \lesssim M_1 \quad (46)$$

which in terms of the bare parameters yields:

$$|A_0| < M_0 \frac{\sqrt{6}}{3 + \sqrt{1 + 8\alpha}} < \sqrt{\frac{3}{8}} M_0 \quad (47)$$

This corresponds to some constraints in the coupling constants as well. From (34) one infers $\kappa/\tilde{g} \lesssim .01$. The S v.e.v. has to be relatively large because of (38), which gives $s/(\sqrt{h_1^2 + h_2^2}) > 20$. From (37) and (47) one derives the constraint, $|\hat{\mu}/\nu| = \lambda/\kappa \gtrsim 5$. On the other hand, (47) also implies $M_0^2 > 24 m_0^2$. In other words, the light singlino scenario corresponds to gaugino masses being the largest soft terms, a “gaugino dominated scenario”. This implies many correlations between sparticle masses.

If the singlino is the LSP, the second lightest neutralino being mostly a \tilde{B} should be quite long-lived. Indeed, its decay into \tilde{s} has to go through its mixing to higgsinos. Then the decay $\tilde{B} \rightarrow \tilde{s}$ is proportional to $g_1^2 (h_1^2 + h_2^2) / s^2 < g_1^2/400$. Conversely, if (47) is not realized, then \tilde{s} will decay into the LSP,

³As a matter of fact, when the mass spectrum of the model is relatively low, the mixings are more important in the neutralino sector, and, besides the singlino, the lightest state can be more like a photino ($\tilde{\gamma}$) than a “bino” (\tilde{B}). But this can be easily incorporated in the discussion that follows where a \tilde{B} -state is assumed for simplicity.

mostly \tilde{B} , with a similar coupling (\tilde{s} would be produced in Higgs or higgsino decays).

Let us now turn to the slepton sector. The lowest lying states are the ν sneutrinos $\tilde{\nu}_e$ and the “right-handed” sleptons, $\tilde{\ell}_R, \ell = e, \mu, \tau$ ⁴. This follows from the assumption of universality for the soft terms. The approximated expressions for the slepton masses as given in the Appendix are

$$\begin{aligned} m_{\tilde{\ell}_R}^2 &= m_0^2 + .15M_0^2 + M_Z^2 \sin^2 \theta_W |\cos 2\beta| \\ m_{\tilde{\nu}}^2 &= m_0^2 + .5M_0^2 - \frac{1}{2}M_Z^2 |\cos 2\beta| \end{aligned} \quad (48)$$

Searches at LEP 1 put a limit of roughly $M_Z^2/4$ on both of them. For the relatively large values of $\tan \beta$ that tend to prevail in the (M+1)SSM $|\cos 2\beta| \approx 1$. With the LEP 1 results on the chargino masses, as pointed out above, one had a bound $2M_0^2 \gtrsim M_Z^2$ and the bounds on $m_{\tilde{\nu}}^2$ gave some useful information. With the LEP 1.5 results, the limit on M_0 implied by (45) is enough to ensure $m_{\tilde{\nu}} > m_{\tilde{\ell}_R}$.

A more interesting issue is provided by the interplay between chargino and slepton searches at LEP 200. In order to compare their masses, we first replace M_0 in (48) in terms of the lightest chargino mass in (43) to obtain

$$m_{\tilde{\ell}_R}^2 \simeq \frac{a}{4(a-1)} m_{\chi^+}^2 + m_0^2 + \frac{M_Z^2}{4} \left(1 + \frac{3}{4a} + \frac{3}{2\sqrt{a} \tan \beta} \right) \gtrsim m_0^2 + \frac{2}{7} M_Z^2 \quad (49)$$

which gives a qualitative explanation of figure (2) in the next section. The difference between $m_{\tilde{\ell}_R}$ and $m_{\chi^+}/2$ is almost a measure of the parameter m_0 in the future searches for these particles at relatively high energies. As a matter of fact, this reverses the situation at LEP 1, where the chargino was expected to be lighter than the selectron. Indeed by comparing (48) and (43), we find that the chargino is always lighter than the selectron if $M_2^2 < M_Z^2/2$, or, equivalently, as $m_{\chi^+}^2 < M_Z^2/3 = (52.5\text{GeV})^2$. This is quite well reproduced by our numerical results.

In particular, in the light singlino scenario, the term m_0^2 can be almost neglected in (49) so that the selectron and chargino masses are strongly correlated.

⁴In a GUT context, the τ superpartners can become considerably splitted and much lighter than the other sleptons, as a consequence of renormalization between the Planck and GUT scales, as noticed in [31]. However in this paper we are assuming $h_t > h_\tau$ at M_{Planck} and we consistently neglect this possibility.

7 Numerical analysis, experimental and theoretical constraints

In this section we describe the numerical procedure employed to produce the figures (1) - (6). As mentioned above, the essential independent parameters of the model are (apart from the lepton and light quark Yukawa couplings and the known gauge couplings) three Yukawa couplings h_t , λ and κ and, under the universality hypothesis at $\Lambda_0 = M_{GUT}$, the three soft parameters M_0 , m_0 and A_0 . Since these are the only dimensionful parameters in the theory and the scale is finally set by the experimental value of M_Z , the true independent parameters are the five dimensionless quantities h_{t_0} , λ_0 , κ_0 , m_0/M_0 and A_0/M_0 .

The numerical results presented here have been obtained by scanning over $\sim 10^6$ points in this five dimensional parameter space. (Here we used a logarithmic measure, but we have checked the results with different measures as well. A lot of scanning of particular regions of the parameter space has been carried out in order to verify the boundaries of the parameter space and the mass ranges, but the results of these scannings are not shown in the figures.) In each case we integrate the one loop renormalization group equations down to the electroweak scale $v = 174$ GeV. To one loop accuracy it is sufficient to use v as the low energy scale, independently from the exact particle masses of $O(v)$. At the one loop level, one can also take advantage of (6) and compute the coefficients in these equations, what saves a lot of computer time to be used for a better scanning.

Actually, also two loop renormalization group equations have been considered in [4]. In this case, however, the low energy scale has to be defined more precisely: The decoupling of particles with masses of $O(v)$ has to be properly taken into account; these masses, in turn, are only known once the Higgs potential (which depends on these masses via the radiative corrections) has been minimized. As a consequence, the numerical procedure becomes much more involved and allows only to study much less points in the parameter space. On the other hand, the corresponding numerical results hardly deviate from ours. Individual points in the parameter space may well lead to somewhat different particle masses, once two loop contributions have been taken into account. Allowed mass ranges and correlations, however, remain practically unchanged. We found it much more important numerically to minimize the full one loop Coleman-Weinberg Higgs potential including the non-logarithmic contributions than to include two loop logarithms.

Having obtained the parameters at low energy it is most convenient to check first the absence of slepton v.e.v.'s according to eq. (24) at the scale $\sim A_e/h_e$. Next we minimize in each remaining case the effective potential (8) including the Coleman-Weinberg radiative corrections (9),(10), numer-

ically. We test, whether the minimum with $\langle S \rangle$, $\langle H_1 \rangle$ and $\langle H_2 \rangle \neq 0$ is the lowest one, and dismiss the corresponding set of parameters otherwise. We calculate $\tan \beta$ and discard the initial conditions that lead to $\tan \beta > 30$ (since we assume $h_t \gg h_b$ in the present work; larger values turn out to be somewhat disfavoured in the model).

In the remaining cases we determine the overall scale of the dimensionful parameters by identifying $\langle H_1^2 \rangle + \langle H_2^2 \rangle$ with $2M_Z^2/(g_1^2 + g_2^2)$, and compute the physical masses of all particles. Then we impose the following experimental constraints: For the top quark pole mass m_t (where we take the leading *QCD* corrections to the pole mass into account [28]) we require $168 \text{ GeV} < m_t < 192 \text{ GeV}$ [6]. Next we impose the LEP 1.5 lower bound on the lightest chargino mass m_{χ^+} : $m_{\chi^+} > 65 \text{ GeV}$ [7]. As a result, nearly all other experimental bounds on new particles turn out to be satisfied automatically, with some exceptions discussed in section 8. Indeed, though the experimental bounds on sleptons, stop, gluinos, as well as on the decays of the Z into neutralinos and Higgs scalars are implemented in our code, these conditions only eliminate a few marginal points in the parameter space. This remarkable property also can be seen from the plots in the next section.

Let us briefly discuss the range of the bare parameters, which turns out to be consistent with our theoretical and experimental constraints. Concerning the Yukawa couplings we first remark that, as in the MSSM, the known range of the top quark mass together with the solution of the RGE for h_t as given in the appendix allows easily to obtain the allowed range for h_{t_0} : $m_t > 168 \text{ GeV}$ leads to $h_{t_0} > 0.468$. The other two bare Yukawa couplings λ_0 and κ_0 turn out to be fairly small, $2.7 \cdot 10^{-3} \lesssim \lambda_0 \lesssim 0.32$ and $1.1 \cdot 10^{-4} \lesssim \kappa_0 \lesssim 0.33$, and relatively closely related, $0.04 \lesssim \kappa_0/\lambda_0 \lesssim 1.14$.

As already remarked below eq. (44), the experimental lower limit on m_{χ^+} implies a lower limit on the soft susy breaking parameter M_0 . The numerical analysis is in good agreement with the approximate analytic result and leads to $M_0 \gtrsim 90 \text{ GeV}$. No strict upper limits (in the absence of fine tuning constraints) on the soft susy breaking parameters have been obtained. The scalar mass term m_0^2 turned out to be unconstrained by our analysis; we assumed, however, $m_0^2 > 0$. The numerical analysis also confirms the allowed range for the third susy breaking parameter A_0 as a function of M_0 and m_0 , eq. (28). The corresponding lower limit on A_0 is a particularity of the (M+1)SSM, since it is required by the need to destabilize the scalar potential in the singlet direction. The correlations between the particle masses and the bare parameters can finally be obtained from the approximate analytic solutions given in sect (6) and the appendix; in table 1 we present the precise numerical parameters and masses for two particular generic cases: one with A_0 negative and a non-singlet LSP, and one with A_0 positive and a singlet LSP.

8 Predictions for the particle spectrum

In order to allow to study the correlations among the particle masses we choose to plot all masses against the lightest chargino mass m_{χ^+} . Each point in these plots corresponds to one of the $\sim 1.5 \cdot 10^3$ points in the parameter space, which satisfy all our theoretical and phenomenological constraints. The density of points in the plots is clearly not uniform; regions of low density (if not completely empty and hence forbidden), typically towards larger particle masses, correspond to regions where more and more fine tuning is required. We will not, however, employ quantitative “fine tuning constraints” in this paper in order to constrain the particle masses from above; a reader, who is interested in “probable particle masses”, can obtain them by investigating the relative densities in our plots. Let us first consider the gluino mass M_3 , fig. 1. As already noted in eq. (44), given the present experimental bounds, m_{χ^+} and M_3 turn out to be strongly correlated. Fig. 1 agrees well with the approximate analytic relation (44), and one sees that the lower experimental bound on m_{χ^+} turns into a lower bound $M_3 \gtrsim 260$ GeV on the gluino mass within our model. For large masses, the ratio between the lightest chargino and the gluino is close to g_2^2/g_3^2 as predicted by the chargino being a wino, but slightly smaller as the parameters in the chargino mass matrices are dynamically correlated (as discussed in section 6).

Next we turn to the slepton masses. The lightest charged “right-handed” slepton mass $m_{\tilde{\ell}_R}$ is plotted against m_{χ^+} in fig. 2. We see that $m_{\chi^+} > 65$ GeV implies $m_{\tilde{\ell}_R} > 55$ GeV in our model. In most cases, as noted below (49), the charged slepton mass $m_{\tilde{\ell}_R}$ has the tendency to be smaller than m_{χ^+} (except for large values of the bare scalar mass m_0), although it always satisfies $m_{\tilde{\ell}_R} \gtrsim m_{\chi^+}/2$ in agreement with the analytic approximation (49). In fig. 3 we plot the sneutrino mass $m_{\tilde{\nu}}$ against m_{χ^+} . Given $m_{\chi^+} > 65$ GeV, the LEP 1 lower limit on $m_{\tilde{\nu}}$ only eliminates a tiny additional corner in the parameter space.

The neutral scalar Higgs sector has already been discussed in detail in ref. [5], in particular with respect to future experiments at LEP 2. Although in [5] only the LEP 1 bound on the chargino mass m_{χ^+} had been taken into account, the results concerning the neutral Higgs sector remain essentially unchanged. Therefore we briefly repeat only the essential features. In order to take the experimental constraints on neutral Higgs bosons properly into account both their masses *and* their couplings to the Z bosons have to be evaluated. In fact, the negative LEP 1 results on neutral CP-even Higgs scalars [6] eliminate only a tiny region of the parameter space of the present model, corresponding to $m_h < 58$ GeV and a coupling hZZ as large as in the non-supersymmetric standard model. On the other hand, a large region with smaller values of m_h , but small couplings hZZ remains unconstrained by LEP 1. In this region the lightest CP-even Higgs scalar is essentially a gauge

singlet and hence decoupled. In view of this possibility the experimental searches for and the theoretical upper limits on the masses of the lightest CP-even Higgs scalar have to be turned into considerations of the “lightest visible CP-even Higgs scalar”. Fortunately it turns out within the present model [1, 3, 29], that upper limits exist also on the lightest visible CP-even Higgs scalar (which could be the second lightest), varying from 140 to 160 GeV for gluino masses (as a measure of the susy breaking scale) from 1 to 3 TeV. Similar complications arise also in the CP-odd Higgs sector, which contains a gauge singlet state as well. Here no upper limit can be derived, and we just remark that a visible CP-odd Higgs scalar below 130 GeV is impossible within the present model and the present experimental constraints on m_{χ^+} .

As in the MSSM the mass of the visible (non-singlet) CP-odd Higgs scalar is actually just somewhat below the mass m_{H^+} of the charged Higgs; cf. the upper left entry of the CP-odd mass matrix eq. (15) and eq. (16). In fig. 4 we plot m_{H^+} against m_{χ^+} , and we see that the present lower limit on m_{χ^+} implies $m_{H^+} > 160 \text{ GeV}$ (increasing rapidly with increasing lower limits on m_{χ^+}).

The range of $\tan \beta$ is fairly restricted, and depends strongly on the sign of the bare susy breaking parameter A_0 : for $A_0 > 0$ we have $\tan \beta < -2.6$, whereas for $A_0 < 0$ we find both signs, but large absolute values for $\tan \beta$: $\tan \beta < -6.5$ or $\tan \beta > 8.7$. Since these inequalities hardly depend on the mass of the chargino, a figure does not provide additional information.

Next we turn to the squarks. Because of renormalization effects between M_{GUT} and M_Z (cf. the appendix) the lightest stop eigenstate is the lightest of all squarks; subsequently we concentrate on this particle. In fig. 5 we plot its mass m_{T_1} against m_{χ^+} , and we see that the present lower limit on m_{χ^+} implies $m_{T_1} > 170 \text{ GeV}$. A possible “supersymmetric” top quark decay mode is thus practically excluded within the present model.

Finally we consider the neutralino sector. As discussed in chapter (6), two different scenarios are possible within the present model, depending on the mass of the nearly pure singlino: In the case of a heavy singlino, the two lightest neutralino states are a practically pure bino with a mass M_1 and a practically pure wino with a mass $M_2 \sim 2M_1$. The numerical procedure confirms this approximate analytic result to a very high accuracy. Since furthermore the chargino mass m_{χ^+} is close to M_2 , cf. eq. (44), the two lightest neutralino masses can easily be obtained as a function of m_{χ^+} and a figure is of no further use. Here the LSP is, of course, the bino, and the supersymmetric decays of all sparticles will proceed as in the MSSM with a suitable set of parameters.

The case of a light singlino is actually more interesting. From the numerical analysis we find, that now the second and third neutralinos correspond to the above mentioned nearly pure bino and wino states. In fig. 6 we plot the mass of the lightest singlino, m_{l_s} , against the bino mass M_1 (for those

parameters where $m_{l_s} < M_1$). Now supersymmetric decays of all sparticles will start as in the MSSM, until the bino state is produced. (A direct decay into the singlino LSP will be heavily suppressed due to its tiny coupling.) Finally the bino will decay into the singlino LSP, producing an additional cascade, whose consequences on experimental susy searches still have to be worked out in more detail.

9 Conclusions and outlook

In the present paper we have presented an exhaustive overview over the parameter space and the particle spectra, which are consistent with the correct vacuum structure and present experimental constraints, within the (M+1)SSM under the universality hypothesis. Since the scalar potential and the corresponding minimization conditions differ considerably from the MSSM due to the presence of the additional singlet superfield, the outcome of this analysis was far from predictable. We have seen that still a large region in the parameter space consistent with all constraints exists. This region is characterized, however, by a) small values of the new Yukawa couplings λ and κ , b) a large value of the scalar singlet $v\bar{v}$, c) a strong tendency of the singlet states to decouple from the rest of the spectrum. In spite of the complexity of the model this region allows for fairly accurate analytical approximations to the vacuum minimization conditions and particle masses, which we have worked out and presented in some detail.

The near decoupling of the singlet states leads to a particle spectrum, which is close to the MSSM for a suitable set of the corresponding parameters. Our figures show strong correlations or inequalities among the particle masses, which allow for experimental falsifications of our underlying hypotheses. For instance, as in the MSSM with the universality hypothesis, sparticles are not light enough to play an important role for the radiative corrections to $R_{b\bar{b}}$ [30]. Only the Higgs boson, the lightest chargino, sleptons and neutralinos could be light enough to be discovered at LEP 2; gluinos, squarks and charged or CP-odd Higgs scalars are necessarily too heavy in our model.

Our approximate analytic results allow to translate future possibly negative sparticle searches into constraints on the soft susy breaking parameters. Obvious are lower limits on the universal gaugino mass M_0 from negative chargino searches (cf. eq. (44)) and, of course, negative gluino searches. From eqs. (50), one can furthermore easily deduce excluded regions in the $m_0 - M_0$ plane from negative “right-handed” slepton and sneutrino searches. These relations are actually not different from the MSSM. Eq. (28), however, allows to turn these constraints on m_0 and M_0 into constraints on A_0 , which is a particular feature of the (M+1)SSM.

If future sparticle searches turn out to be successful, and the mass pattern predicted by our model turns out to be confirmed, the question arises whether the model can be distinguished from the MSSM with corresponding parameters. The answer depends on the corresponding parameters of the $(M+1)$ SSM. First, there still exist small corners in the parameter space, where mixing with the singlet states either in the neutral Higgs sector or in the neutralino sector could be possible; in this case the couplings of the corresponding visible particles could be substantially and hence measurably smaller than in the MSSM. A more likely possibility - but by no means certain - is the singlino LSP scenario. As discussed in the previous section, in this case sparticle decays will produce an additional cascade with respect to the MSSM. This scenario deserves further phenomenological investigations.

A Appendix

In this Appendix we list the analytic solutions of the RGE for soft susy breaking terms in the approximation where the dependence on all Yukawa couplings but the top one, h_t , are neglected.

Also, flavour mixing is neglected in these expressions (see [32]) for solutions that fully take family mixing into account). However, for the sake of generality, universality is *not* assumed for the soft terms at the unification scale, Λ_0 . All quantities are defined at the scale Λ (unless stated otherwise) and the boundary conditions at the scale Λ_0 , are generally denoted as $X_0 = X(\Lambda_0)$. We define the following quantities:

$$\begin{aligned}
 t &= \frac{1}{16\pi^2} \ln \frac{\Lambda_0}{\Lambda} \\
 \Pi_{(i)} &= \prod_{\alpha=1}^3 \left(\frac{g_\alpha^2}{g_{\alpha 0}^2} \right)^{\frac{2C_\alpha^{(i)}}{b_\alpha}} \\
 J &= \Pi_{(u)}^{-1}(t) \int_0^t \Pi_{(u)}(t') dt'
 \end{aligned} \tag{50}$$

The index $\alpha = 1, 2, 3$, refers to the $U(1)$, $SU(2)$ and $SU(3)$ gauge groups, respectively, and $C_\alpha^{(i)}$ is the sum of the their quadratic Casimir eigenvalues for the three fields in the i -th Yukawa coupling. We replace the integral J by the value h_{crit} of h_t at the scale Λ corresponding to a Landau pole at Λ_0 , by defining

$$\frac{1}{h_{\text{crit}}^2} = 12J \qquad \rho = \frac{h_t^2}{h_{\text{crit}}^2} \tag{51}$$

The solutions for the Yukawa coupling are then as follows

$$\begin{aligned}
 \lambda^2 &= \lambda_0^2 \Pi_{(\lambda)} (1 - \rho)^{1/2} \\
 h_t^2 &= h_{t_0}^2 \Pi_{(u)} (1 - \rho) \\
 h_{c(u)}^2 &= h_{c(u)0}^2 \Pi^{(u)} (1 - \rho)^{1/2} \\
 h_b^2 &= h_{b_0}^2 \Pi_{(d)} (1 - \rho)^{1/6} \\
 h_{s(d)}^2 &= h_{s(d)0}^2 \Pi_{(d)} \\
 h_\ell^2 &= h_{\ell_0}^2 \Pi_{(\ell)} \quad (\ell = e, \mu, \tau) \\
 \kappa^2 &= \kappa_0^2
 \end{aligned} \tag{52}$$

The soft trilinear terms are as follows:

$$\begin{aligned}
A_\lambda &= A_{\lambda_0} - \frac{1}{2}\rho(A_{t_0} + \xi M_0) + 2M_0t(3g_2^2 + g_1^2) \\
A_\kappa &= A_{\kappa_0} \\
A_t &= A_{t_0} - \rho(A_{t_0} + \xi M_0) + 2M_0t\left(\frac{16}{3}g_3^2 + 3g_2^2 + \frac{13}{9}g_1^2\right) \\
A_{c(u)} &= A_{c(u)0} - \frac{1}{2}\rho(A_{t_0} + \xi M_0) + 2M_0t\left(\frac{16}{3}g_3^2 + 3g_2^2 + \frac{13}{9}g_1^2\right) \\
A_b &= A_{b_0} - \frac{1}{6}\rho(A_{t_0} + \xi M_0) + 2M_0t\left(\frac{16}{3}g_3^2 + 3g_2^2 + \frac{1}{9}g_1^2\right) \\
A_{s(d)} &= A_{s(d)0} + 2M_0t\left(\frac{16}{3}g_3^2 + 3g_2^2 + \frac{1}{9}g_1^2\right) \\
A_{\tau(\mu,e)} &= A_{\tau(\mu,e)0} + 2M_0t(3g_2^2 + 3g_1^2) \\
\xi &= \left(\frac{t}{J} - 1\right) = (12h_{\text{crit}}^2 t - 1) \tag{53}
\end{aligned}$$

Soft supersymmetry breaking scalar masses can also be written in terms of ρ, t and J (or ξ), as follows:

$$\begin{aligned}
m_S^2 &= m_{S0}^2 \\
m_1^2 &= m_{10}^2 + g_1^2 t s_0 + 2\gamma_L t M_0^2 \\
m_2^2 &= m_{20}^2 - \frac{3\rho}{2}\overline{m}_0^2 - \frac{\rho}{2}K - g_1^2 t s_0 + 2\gamma_L t M_0^2 \\
m_T^2 &= m_{T0}^2 - \rho\overline{m}_0^2 - \frac{\rho}{3}K + \frac{4}{3}g_1^2 t s_0 + 2\gamma_U t M_0^2 \\
m_{Q_3}^2 &= m_{Q_30}^2 - \frac{\rho}{2}\overline{m}_0^2 - \frac{\rho}{6}K - \frac{1}{3}g_1^2 t s_0 + 2\gamma_Q t M_0^2 \\
m_B^2 &= m_{B0}^2 - \frac{2}{3}g_1^2 t s_0 + 2\gamma_D t M_0^2 \\
m_{U_i}^2 &= m_{U_i0}^2 + \frac{4}{3}g_1^2 t s_0 + 2\gamma_U t M_0^2 \\
m_{Q_i}^2 &= m_{Q_i0}^2 - \frac{1}{3}g_1^2 t s_0 + 2\gamma_Q t M_0^2 \\
m_{D_i}^2 &= m_{D_i0}^2 - \frac{2}{3}g_1^2 t s_0 + 2\gamma_D t M_0^2 \\
m_{L_j}^2 &= m_{L_j0}^2 + g_1^2 t s_0 + 2\gamma_L t M_0^2 \\
m_{E_j}^2 &= m_{E_j0}^2 - 2g_1^2 t s_0 + 2\gamma_E t M_0^2 \\
\gamma_L &= 3g_2^2(1 - g_2^2 t) + g_1^2(1 - 11g_1^2 t) \\
\gamma_U &= \frac{16}{3}g_2^2(1 + 3g_3^2 t) + \frac{16}{9}g_1^2(1 - 11g_1^2 t) \\
\gamma_Q &= \frac{16}{3}g_3^2(1 + 3g_3^2 t) + 3g_2^2(1 - g_2^2 t) + \frac{1}{9}g_1^2(1 - 11g_1^2 t)
\end{aligned}$$

$$\begin{aligned}
\gamma_D &= \frac{16}{3}g_3^2(1+3g_3^2t) + \frac{4}{9}g_1^2(1-11g_1^2t) \\
\gamma_E &= 4g_1^2(1-11g_1^2t) \\
s_0 &= \left[m_{H_2}^2 - m_{H_1}^2 + \sum_i (m_{Q_i}^2 + m_{D_i}^2 + m_{E_i}^2 - m_{L_i}^2 - 2m_{U_i}^2) \right]_{t=0} \\
\overline{m}_0^2 &= \frac{1}{3}(m_2^2 + m_T^2 + m_Q^2)_{t=0} \\
K &= (1-\rho)(A_{t_0} + \xi M_0)^2 - \xi^2 M_0^2 + \\
&\quad + 2\left(\frac{16}{3}g_3^2 + 3g_2^2 + \frac{13}{9}g_1^2\right)(\xi+1)tM_0^2
\end{aligned} \tag{54}$$

Finally, let us recall that the renormalization effects on the effective variables \hat{B} and $\hat{\mu}$ are easily obtained by taking the limit in which the singlet fields are decoupled at its classical value. Then,

$$\begin{aligned}
\hat{B} &= A_\lambda + \nu = \hat{B}_0 - \frac{1}{2}\rho(A_{t_0} + \xi M_0) + 2M_0t(3g_2^2 + g_1^2) \\
\hat{\mu}^2 &= \lambda^2 s^2 = \hat{\mu}_0^2 \Pi^{(\lambda)}(1-\rho)^{1/2}
\end{aligned} \tag{55}$$

References

- [1] J. Ellis, J. F. Gunion, H. E. Haber, L. Roszkowski, F. Zwirner, *Phys. Rev.* **D 39** (1989) 844;
L. Durand and J. L. Lopez, *Phys. Lett.* **B 217** (1989) 463;
M. Drees, *Int. J. Mod. Phys.* **A 4** (1989) 3635.
- [2] U. Ellwanger, M. Rausch de Traubenberg, C. A. Savoy, *Phys. Lett.* **B 315** (1993) 331.
- [3] T. Elliott, S. F. King and P. L. White, *Phys. Lett.* **B 305** (1993) 71;
T. Elliott, S. F. King and P. L. White, *Phys. Lett.* **B 314** (1993) 56;
T. Elliott, S. F. King, P. L. White, *Phys. Rev.* **D 49** (1994) 2435.
- [4] S. F. King and P. L. White, *Phys. Rev.* **D 52** (1995) 4183.
- [5] U. Ellwanger, M. Rausch de Traubenberg and C. A. Savoy, *Z. Phys.* **C 67** (1995) 665.
- [6] R. M. Barnett et al., *Phys. Rev.* **D 54** (1996) 1.
- [7] Aleph Collaboration, *Phys. Lett.* **B 373** (1996) 246.
- [8] U. Ellwanger, *Phys. Lett.* **B 303** (1993) 271.
- [9] G. F. Giudice and A. Masiero, *Phys. Lett.* **B 206** (1988) 480.
- [10] H. -P. Nilles, M. Srednicki, D. Wyler, *Phys. Lett.* **B 120** (1983) 346.
- [11] H. Nilles, M. Srednicki, and D. Wyler, *Phys. Lett.* **B 124** (1983) 337.
A. Lahanas, *Phys. Lett.* **B 124** (1983) 341.
- [12] U. Ellwanger, *Phys. Lett.* **B 133** (1983) 187;
J. Bagger, E. Poppitz, *Phys. Rev. Lett.* **71** (1993) 2380;
J. Bagger, E. Poppitz, L. Randall, *Nucl. Phys.* **B 455** (1995) 59.
- [13] S. A. Abel, S. Sarkar and P. L. White, *Nucl. Phys.* **B 454** (1995) 663,
S. A. Abel, preprints hep-ph 9603301 and hep-ph 9609323.
- [14] A. Pomarol, *Phys. Lett.* **B 287** (1992) 331.
- [15] J. Romão, *Phys. Lett.* **B 173** (1986) 309.
- [16] K. S. Babu and S. M. Barr, *Phys. Rev.* **D49** (1994) 2156.
- [17] Y. Okada, M. Yamaguchi and T. Yanagida, *Progr. Theor. Phys. Lett.* **85** (1991) 1, *Phys. Lett.* **B 262** (1991) 54.
J. Ellis, G. Ridolfi and F. Zwirner, *Phys. Lett.* **B 257** (1991) 83, *Phys. Lett.* **B 262** (1991) 474.

- H. Haber and R. Hempfling, *Phys. Rev. Lett.* **66** (1991) 1815.
P. Chankowski, S. Pokorski and J. Rosiek, *Phys. Lett.* **B 274** (1992) 191.
- [18] J. A. Casas, J. R. Espinosa, M. Quiros and A. Riotto, *Nucl. Phys.* **B 436** (1995) 3.
M. Carena, J. Espinosa, M. Quiros, C. Wagner, *Phys. Lett.* **B 335** (1995) 209.
- [19] U. Ellwanger, M. Rausch de Traubenberg, *Z. Phys.* **C 53** (1992) 521;
P. Binetruy and C. A. Savoy, *Phys. Lett.* **B 277** (1992) 453.
J. R. Espinosa and M. Quiros, *Phys. Lett.* **B 279** (1992) 92;
G. Kane, C. Kolda and J. Wells, *Phys. Rev. Lett.* **70** (1993) 2686;
J. R. Espinosa and M. Quiros, *Phys. Lett.* **B 302** (1993) 51.
U. Ellwanger and M. Lindner, *Phys. Lett.* **B 301** (1993) 365;
- [20] Ph. Brax, U. Ellwanger and C. A. Savoy, *Phys. Lett.* **B 347** (1995) 269.
- [21] J. -P. Derendinger, C. A. Savoy, *Nucl. Phys.* **B 237** (1984) 307.
- [22] J. -M. Frère, D. R. T. Jones, S. Raby, *Nucl. Phys.* **B 222** (1983) 11.
- [23] G. Gamberini, G. Ridolfi and F. Zwirner, *Nucl. Phys.* **B 331** (1990) 331.
- [24] M. Olechowski and S. Pokorski, *Phys. Lett.* **B 214** (1988) 393.
- [25] J. A. Casas, A. Lleyda and C. Muñoz, *Nucl. Phys.* **B 471** (1996) 3.
A. J. Borner, hep-ph/9506409.
- [26] R. Barbieri, S. Ferrara and C. A. Savoy, *Phys. Lett.* **B 119** (1982) 343.
R. Arnowitt, A. Chamseddine and P. Nath, *Phys. Rev. Lett.* **D 49** (1982) 970.
L. Hall, J. Lykken and S. Weinberg, *Phys. Rev.* **D 27**(1983) 2359.
- [27] V. S. Kaplunovski and J. Louis, *Phys. Lett.* **B306** (1993) 269.
R. Barbieri, J. Louis and M. Moretti, *Phys. Lett.* **B312** (1993) 451.
A. Brignole, L. E. Ibáñez and C. Muñoz, *Nucl. Phys.* **B422** (1994) 235.
- [28] R. Tarrach, *Nucl. Phys.* **B 183** (1981) 384.
- [29] J. Kamoshita, Y. Okada and M. Tanaka, *Phys. Lett.* **B 328** (1994) 67.
- [30] J. D. Wells, C. Kolda and G. L. Kane, *Phys. Lett.* **B 338** (1994) 219.
G. L. Kane, R. G. Stuart, J. D. Wells *Phys. Lett.* **B 354** (1995) 350.
D. Garcia and J. Sola, *Phys. Lett.* **B 354** (1995) 335.
P. H. Chankowski and S. Pokorski, *Phys. Lett.* **B 366** (1996) 188.
J. Ellis, J. L. Lopez and D. V. Nanopoulos, *Phys. Lett.* **B 372** (1996) 95.

[31] R. Barbieri, L. Hall and A. Strumia, *Phys. Lett.*

[32] Ph. Brax and C. A. Savoy, *Nucl. Phys. B* **447** (1995) 227.

Figure captions

Figure 1: Gluino mass M_3 versus the chargino mass m_{χ^+} (all in GeV)

Figure 2: Slepton mass $m_{\tilde{\ell}_R}$ versus m_{χ^+}

Figure 3: Sneutrino mass $m_{\tilde{\nu}}$ versus m_{χ^+}

Figure 4: Lightest stop mass m_{T_1} versus m_{χ^+}

Figure 5: Charged Higgs mass m_{H^+} versus m_{χ^+}

Figure 6: Mass of the second lightest neutralino $m_{\chi_2^0}$ versus the mass of the lightest neutralino $m_{\chi_1^0}$ in those cases where χ_1^0 is essentially a singlino

Table caption

Table 1: Parameters and particle masses (in GeV) for two particular cases (with M_{susy} not too large). The three neutral CP even Higgs scalars are denoted by h_1 , h_2 and h_3 (in the order of increasing masses), the two neutral CP odd Higgs scalars by p_1 and p_2 , and the two lightest neutralinos by χ_1^0 and χ_2^0 , respectively. In the first case χ_1^0 is essentially a non-singlet, in the second case it practically a pure singlino.

Table 1

λ_0	$6,89 \cdot 10^{-3}$	$2.68 \cdot 10^{-3}$
κ_0	$2.16 \cdot 10^{-3}$	$1.08 \cdot 10^{-4}$
h_{t_0}	0.470	0.534
M_0	104	116
A_0	- 95.8	11.6
m_0	22	0.6
λ	$7,18 \cdot 10^{-3}$	$2.67 \cdot 10^{-3}$
κ	$2.16 \cdot 10^{-3}$	$1.08 \cdot 10^{-4}$
h_t	0.932	0.966
A_λ	- 46.7	31.8
A_κ	- 95.8	11.6
A_t	- 273	- 256
s	19500	- 53300
$ \tan(\beta) $	8.17	16.0
m_{top}	170	177
M_3	280	313
m_{h_1}	55.1	8.00
singlet component of h_1	.999	1.00
m_{h_2}	101	108
m_{h_3}	156	157
m_{p_1}	110	14.2
m_{p_2}	152	156
m_{H^+}	172	176
$m_{\tilde{\ell}_R}$	63.2	62.9
$m_{\tilde{\nu}}$	46.5	54.8
m_{χ^+}	72.9	65.9
m_{T_1}	179	214
$m_{\chi_1^0}$	42.0	11.5
singlet component of χ_1^0	0.01	1.00
$m_{\chi_2^0}$	71.4	39.1

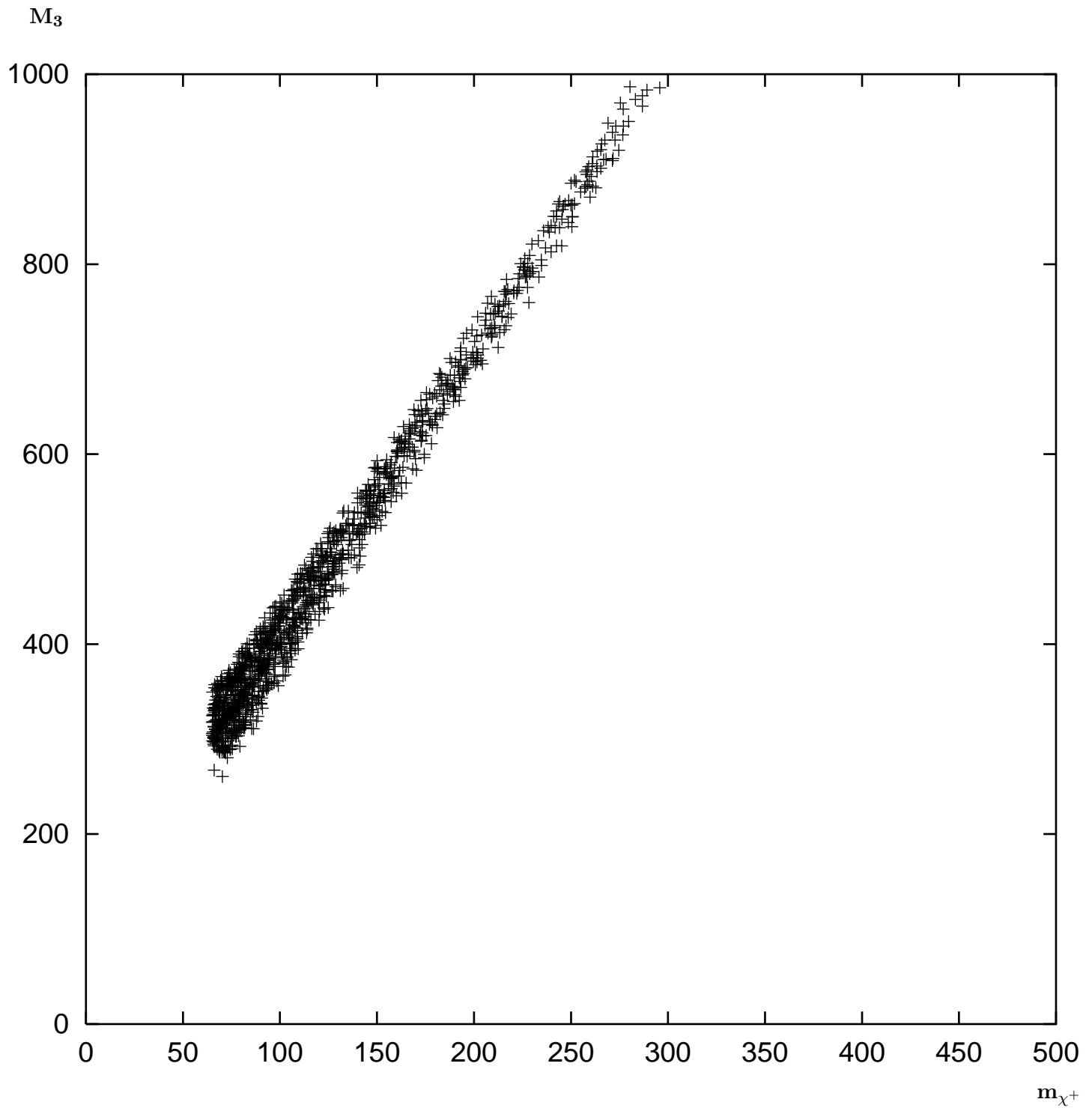


Figure 1

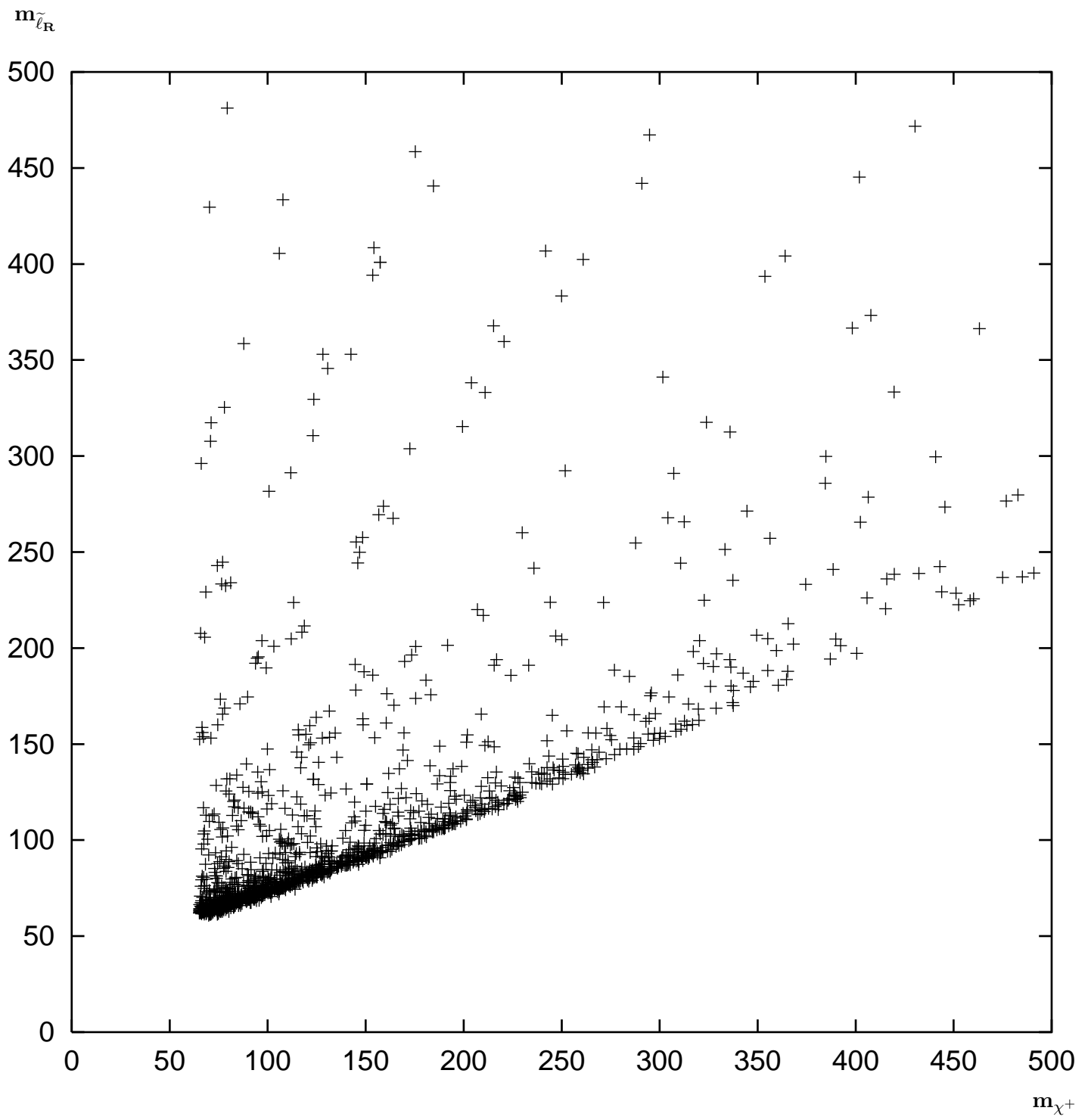


Figure 2

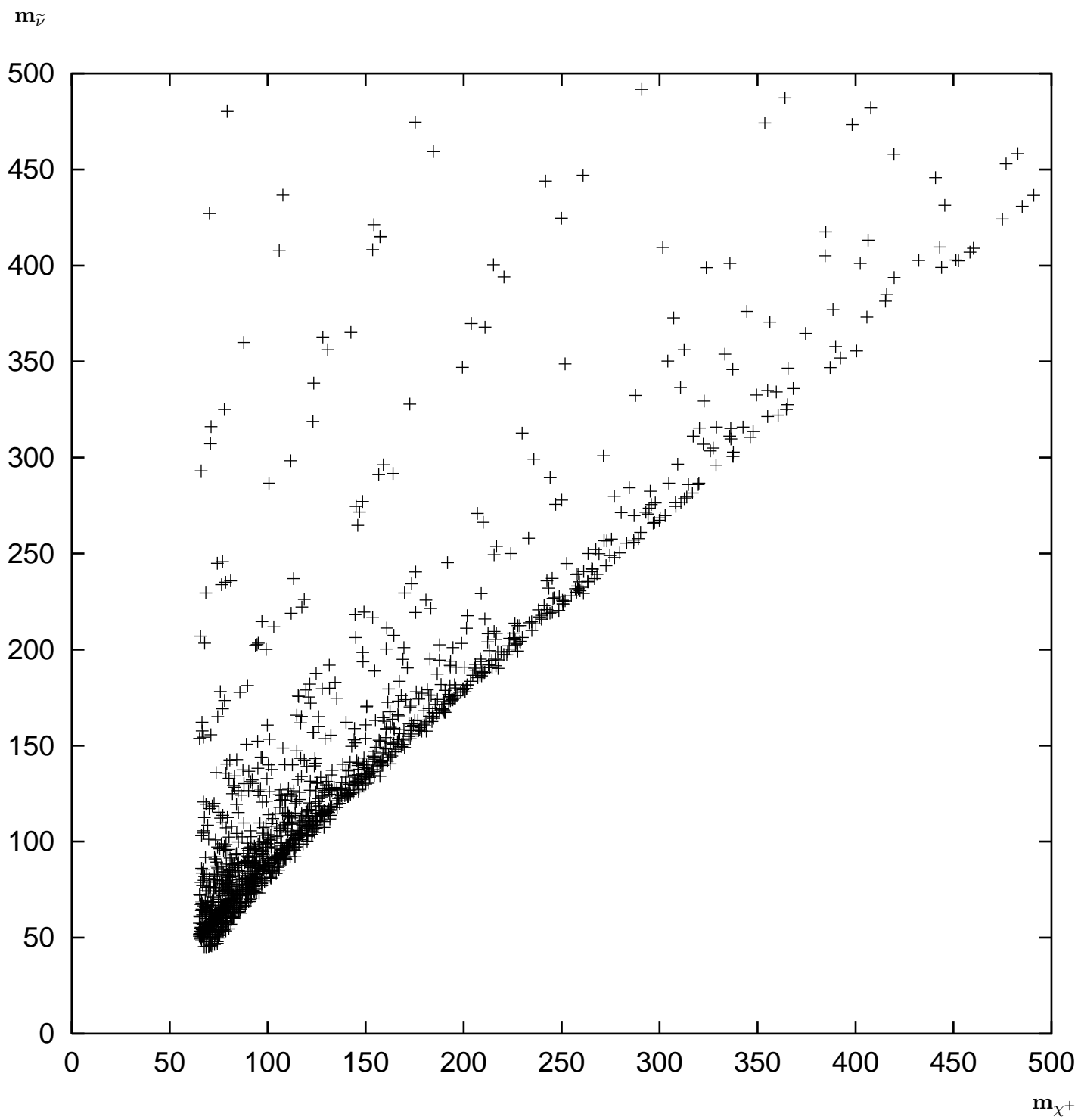


Figure 3

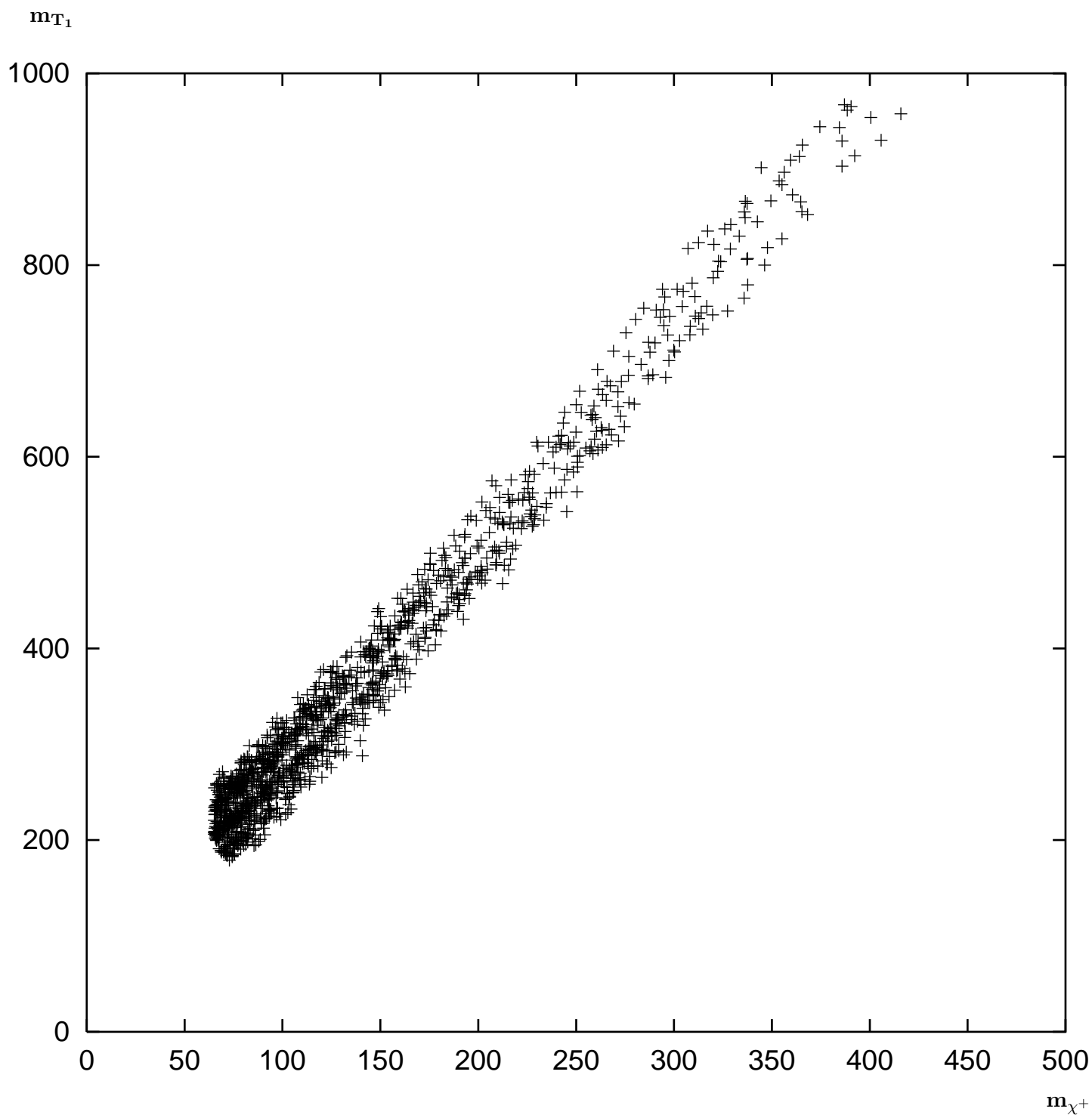


Figure 4

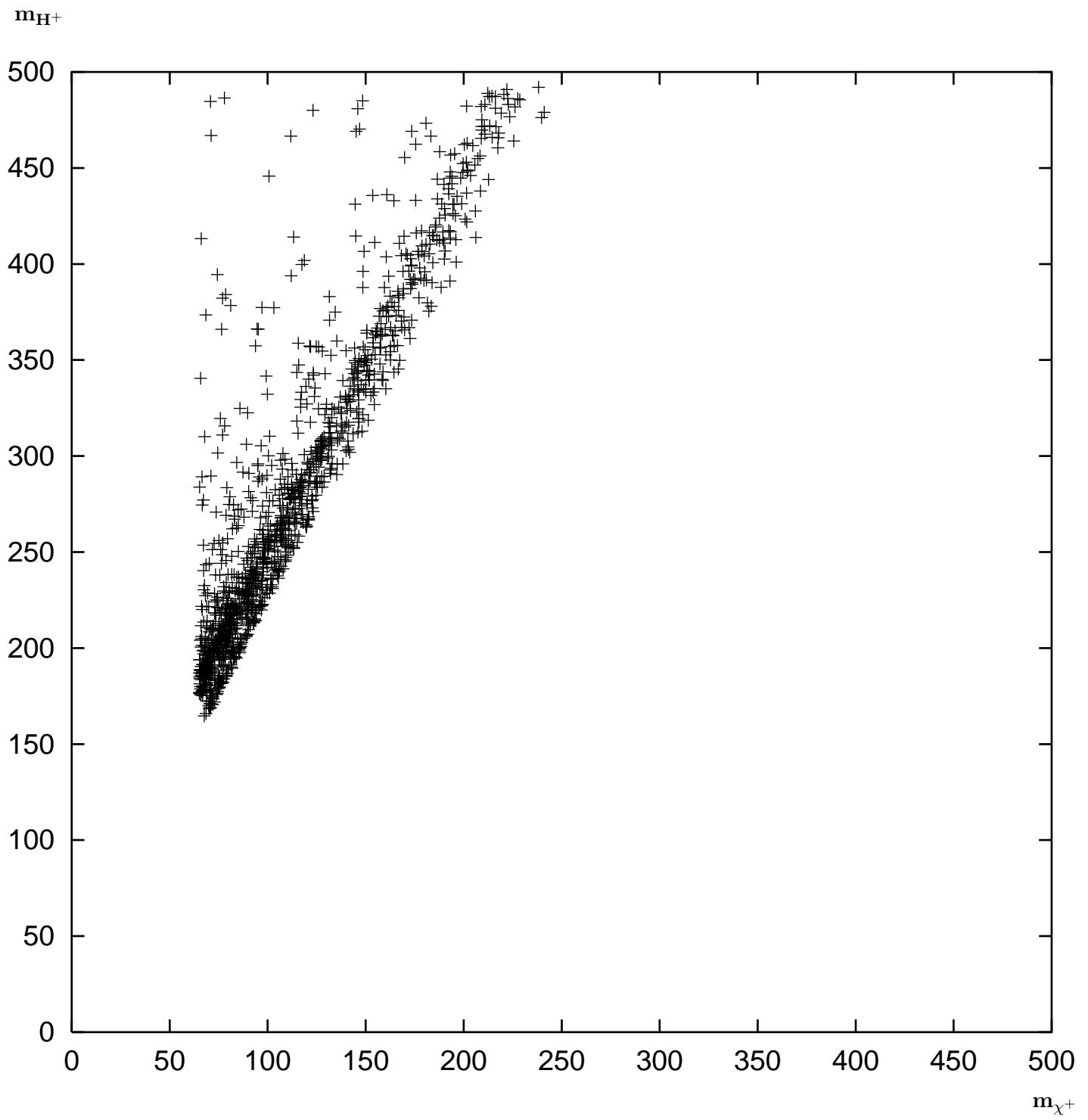


Figure 5

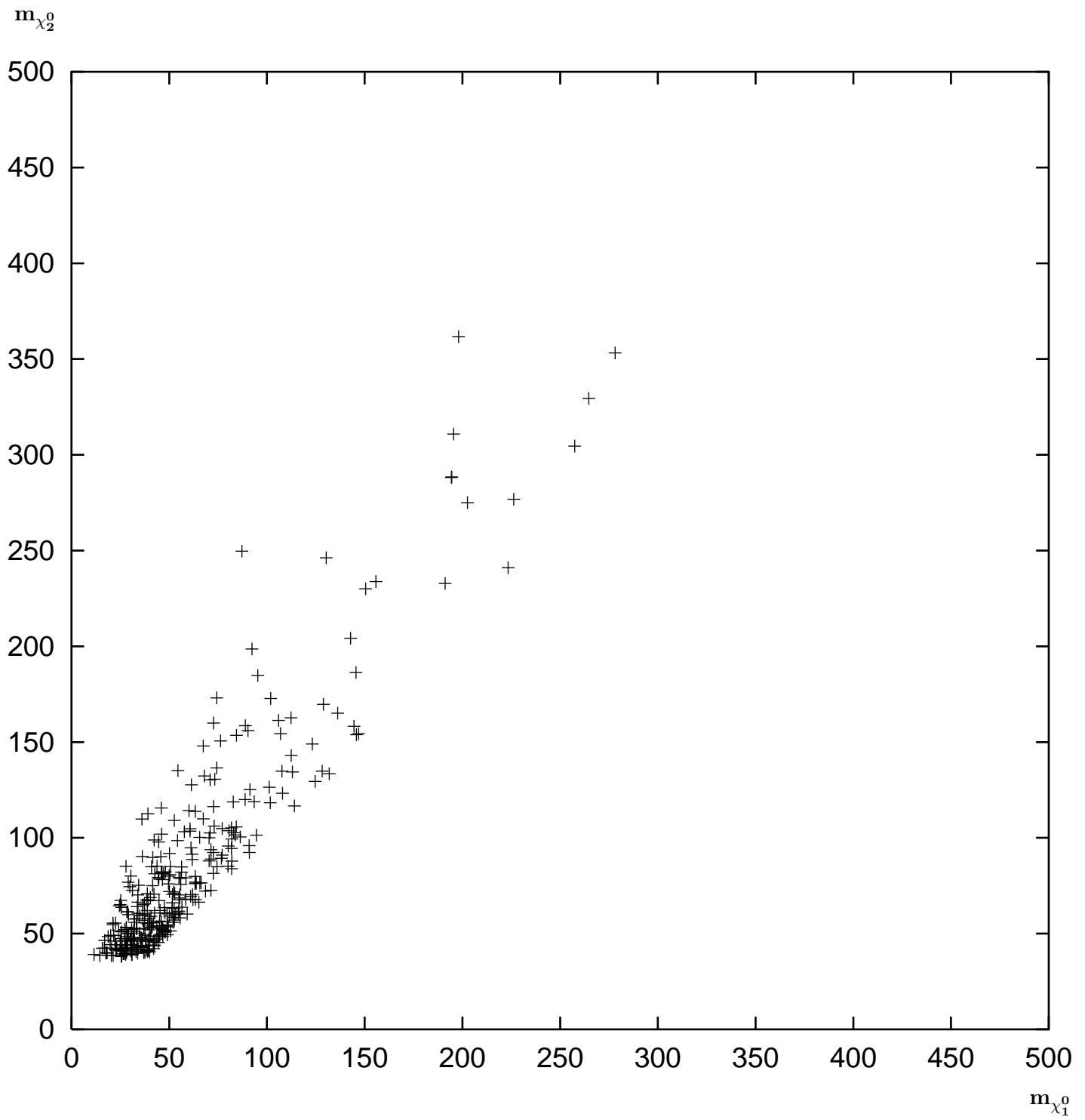


Figure 6